STRUCTURAL CHEMISTRY

ISSN 2053-2296

Received 4 September 2025
Accepted 29 October 2025

Edited by A. Lemmerer, University of the Witwatersrand, South Africa

Keywords: cobalt aminodiphosphine complexes; crystal structure; CSD survey; noncovalent interactions.

CCDC references: 2499418; 2499419

Supporting information: this article has supporting information at journals.iucr.org/c

Structural insights into transition-metal–amino-diphosphine (PNP) complexes bearing $[MCl_n(PNP)_2]$ (M = Co, Ru, Cr or Mo; n = 1 or 2) cores in the solid state

Sizwe J. Zamisa,* Adesola A. Adeleke,* Dunesha Naicker, Holger B. Friedrich and Bernard Omondi

School of Agriculture and Science, Discipline of Chemistry, University of KwaZulu-Natal, Private Bag X54001, Westville, Durban, 4000, South Africa. *Correspondence e-mail: zamisas@ukzn.ac.za, adelekea@ukzn.ac.za

The molecular structures of two novel cobalt aminodiphosphine (PNP) complexes (**1** and **2**) are reported, namely, bis[bis(diphenylphosphanyl)(pentyl)-amine-κ^2P,P']chloridocobalt(III) di-μ-chlorido-bis[dichloridocobalt(II)], $[CoCl(C_{29}H_{31}NP_2)_2][Co_2Cl_6]$, and bis[bis(diphenylphosphanyl)(propan-2-yl)amine-κ^2P,P']chloridocobalt(III) di-μ-chlorido-bis[dichloridocobalt(II)], $[CoCl(C_{27}H_{27}NP_2)_2][Co_2Cl_6]$, featuring variation in the N-atom substituent, *i.e.* *n*-pentyl in complex **1** and isopropyl in complex **2**. The asymmetric unit of complex **1** contains a five-coordinated cationic $[CoCl\{\kappa^2\text{-}P,P\text{-}(N)\text{-}C_5H_{11}\}_2]^{2+}$ species and a $[Co_2(\mu_2\text{-}Cl)_2Cl_4]^{2-}$ anion, while complex **2** includes a five-coordinated cation $[CoCl\{\kappa^2\text{-}P,P\text{-}(N)\text{-}C_3H_7\}_2]$, half a $[Co_2(\mu_2\text{-}Cl)_2Cl_4]^{2-}$ anion, and disordered diethyl ether and dichloromethane solvent molecules. The impact of ligand-induced strain, particularly due to the small bite angles of the PNP amino-diphosphine ligands, was examined in the context of geometric constraints and their influence on stability and reactivity. A Cambridge Structural Database (CSD) survey, along with a noncovalent interaction (NCI) analysis of the analogous $[TMCl_n(PNP)_2]$ (where TM = transition metal and n = 1 or 2) core, revealed an inverse correlation between P—TM—P bite angles and N···TM contact distances. This correlation is attributed to the influence of the van der Waals radius of the metal: smaller metals allow wider bite angles and stronger N···TM contacts, whereas larger metals favour narrower bite angles and longer N···TM distances. NCI analysis indicated significant steric repulsion at the TM···N contacts, reflecting strain imposed by ligand geometry. A comparison of sign(λ_2)ρ eigenvalues suggests that Mo—P bonds exhibit weaker attractive interactions relative to Co—P and Ru—P bonds, with Cr—P bonds being the weakest. These findings provide pointers to structural and electronic factors governing coordination in PNP-ligated transition-metal complexes, offering rational design and catalytic and material applications.

1. Introduction

Nitrogen-containing phosphines and phosphinites are ligands that have attracted significant attention in transition-metal coordination chemistry over the years (Hierso *et al.*, 2003; Cotton & Hong, 1992; Mayer & Kaska, 1994; Munzeiwa *et al.*, 2020). Aminodiphosphine derivatives, for instance, are versatile ligands, with the potential to be made more flexible by introducing alkyl chains (Blann *et al.*, 2005; Olding *et al.*, 2024) or more rigid by using fixed groups between the P atoms (Overett *et al.*, 2005; Beims *et al.*, 2023). Typically, amino-diphosphine ligands coordinate to metal centres *via* P-donor atoms, often excluding the N atom. However, the coordination behaviour and structural features of these ligands can be influenced by modifying the groups attached to the P or N

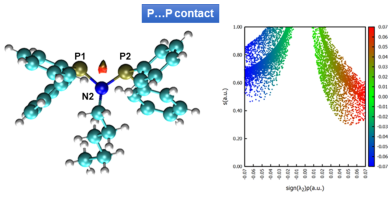

Table 1
Experimental details.

Experiments were carried out at 100 K with Mo $K\alpha$ radiation using a Bruker SMART APEXII area-detector diffractometer. Absorption was corrected for by multi-scan methods (*SADABS*; Bruker, 2009). H-atom parameters were constrained.

	1	**2**
Crystal data		
Chemical formula	$[CoCl(C_{29}H_{31}NP_2)_2][Co_2Cl_6]$	$[CoCl(C_{27}H_{27}NP_2)_2][Co_2Cl_6]$
M_r	1336.01	1279.90
Crystal system, space group	Triclinic, $P\overline{1}$	Monoclinic, $P2_1/c$
a, b, c (Å)	11.5114 (4), 12.6404 (4), 20.7858 (7)	12.2179 (2), 15.4508 (2), 30.4455 (5)
α, β, γ (°)	89.481 (2), 82.999 (2), 68.324 (2)	90, 97.070 (1), 90
V (Å^3)	2787.57 (17)	5703.69 (15)
Z	2	4
μ (mm^{-1})	1.38	1.34
Crystal size (mm)	0.35 × 0.22 × 0.14	0.40 × 0.18 × 0.14
Data collection		
T_{min}, T_{max}	0.640, 0.746	0.672, 0.746
No. of measured, independent and observed $[I \geq 2\sigma(I)]$ reflections	74041, 13808, 11199	131209, 14218, 11950
R_{int}	0.042	0.029
$(\sin \theta/\lambda)_{max}$ (Å^{-1})	0.667	0.669
Refinement		
$R[F^2 > 2\sigma(F^2)]$, $wR(F^2)$, S	0.040, 0.113, 1.06	0.030, 0.077, 1.05
No. of reflections	13808	14218
No. of parameters	691	629
No. of restraints	242	96
$\Delta\rho_{max}$, $\Delta\rho_{min}$ (e Å^{-3})	1.13, −0.63	0.50, −0.35

Computer programs: *COSMO* (Bruker, 2009), *SAINT-Plus* (Bruker, 2009), *SHELXS* (Sheldrick, 2008), *olex2.refine* (Bourhis *et al.*, 2015), *OLEX2* (Dolomanov *et al.*, 2009) and *PLATON* (Spek, 2020).

atoms, enabling bridging or chelating coordination modes (Zhao *et al.*, 2018; Smith, 2022), and broadens their applications in coordination chemistry (Konrath *et al.*, 2019; Vasilenko *et al.*, 2016; Chirdon *et al.*, 2021).

Transition-metal complexes bearing $[MCl_n(PNP)_2]$ (M = Co, Ru, Cr or Mo; n = 1 or 2) cores in the literature seem to be understudied, especially considering structural features arising from ligand coordination, particularly ligand strain in the P—N—P backbone (Kim *et al.*, 2017; Fliedel *et al.*, 2016; Ogawa *et al.*, 2013; Aydemir *et al.*, 2011; Naicker *et al.*, 2022; Naktode *et al.*, 2014; Gaw *et al.*, 2000; Stennett *et al.*, 2012; Balakrishna *et al.*, 2003; Slawin *et al.*, 2004). While the existing literature predominantly focuses on synthesis (Slawin *et al.*, 2004), catalytic performance (Naicker *et al.*, 2022; Aydemir *et al.*, 2011; Ogawa *et al.*, 2013) and basic structural parameters (Gaw *et al.*, 2000; Fliedel *et al.*, 2016; Balakrishna *et al.*, 2003; Slawin *et al.*, 2004), the explicit effects of ligand-induced strain, particularly from small bite angles inherent in these aminodiphosphine ligands, remain inadequately explored. Notably, significant bite-angle contractions – reported as low as ∼69° in Ru^{II} complexes (Naicker *et al.*, 2022; Balakrishna *et al.*, 2003) and ∼71° in Co complexes (Fliedel *et al.*, 2016) – indicate the substantial strain imposed by these ligands, which likely influences both electronic and steric environments around the metal centres. However, only a few studies explicitly correlate these geometric constraints with broader chemical reactivity or stability implications (Ogawa *et al.*, 2013; Fliedel *et al.*, 2016). Moreover, the interplay between such structural constraints and the van der Waals radii of central transition metals, which could further modulate metal–ligand interactions and catalytic outcomes, has rarely been addressed explicitly.

In this article, two new crystal structures of cobalt aminodiphosphine PNP complexes (**1** and **2**; Scheme 1) are reported featuring variation of the N-atom substituent, *i.e.* *n*-pentyl in complex **1** and isopropyl in complex **2**, allowing us to evaluate the effect of different N-atom substituents on the behaviour of the PNP ligand. A Cambridge Structural Database (CSD; Groom *et al.*, 2016) survey of complexes bearing $[MCl_n(PNP)_2]$ substructures was also used to gain insights into the correlation between metal–ligand geometric bond parameters and metal ion sizes. Finally, noncovalent interaction (NCI) analysis was used to investigate the strain of the aminodiphosphine ligands along the P—N—P backbone caused by the various substituents and metal ions. With this in mind, investigation of ligand-strain effects and associated steric-electronic consequences in $[MCl_n(PNP)_2]$ complexes represents a significant research gap, promising to yield valuable insights into the structure–reactivity relationships critical for their application in catalysis and materials science (Fliedel *et al.*, 2016; Ogawa *et al.*, 2013; Naicker *et al.*, 2022).

2. Experimental

2.1. Materials and equipment

All experiments were performed using standard Schlenk techniques under inert conditions in moisture-free reaction glassware with anhydrous solvents. All solvents were of analytical grade. To render the reaction glassware moisture

free, they were heated with a heat gun, followed by cycles of vacuum and nitrogen purges. The solvents utilized were dry unless otherwise stated. Diethyl ether and hexane were distilled from sodium benzophenone under nitrogen. Dichloromethane was distilled from P_2O_5 and ethanol from magnesium turnings. Complexes **1** and **2** were synthesized

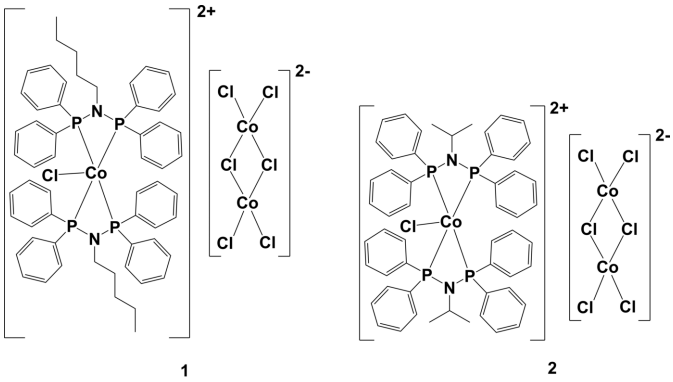

following the literature procedure of Naicker *et al.* (2015). Crystals of **1** and **2** were grown by the vapour diffusion of diethyl ether into a solution of the complexes in dichloromethane at room temperature to give blue crystals for **1** and **2**.

2.2. Crystal structure analyses

Crystal data, data collection and structure refinement details are summarized in Table 1. All H atoms were positioned geometrically and allowed to ride on their respective parent atoms. All H atoms were refined isotropically. The disordered *n*-pentyl group was modelled with split occupancies, with the major component having a site-occupancy factor of 0.55 (3). In complex **2**, a solvent mask was calculated and 218 electrons were found in a volume of 830 Å^3 in two voids per unit cell. This is consistent with the presence of 1 $C_4H_{10}O$ and 0.25 CH_2Cl_2 molecules per asymmetric unit, which account for 42 and 10 electrons per unit cell, respectively.

Table 2
Selected bond lengths (Å) and angles (°) in the solid-state structures of complexes **1** and **2**.

	1	**2**
Bond lengths		
Co1—P1	2.2495 (6)	2.2239 (6)
Co1—P2	2.2514 (6)	2.2259 (6)
Co1—P3	2.2590 (6)	2.2654 (5)
Co1—P4	2.2480 (6)	2.2913 (5)
Co1—Cl1	2.2305 (6)	2.2400 (5)
Co2—Cl2	2.2469 (7)	2.2315 (6)
Co2—Cl3	2.2292 (7)	2.2274 (6)
Co2—Cl4	2.3412 (7)	2.3398 (6)
Bond angles		
P1—Co1—P2	71.35 (2)	71.16 (2)
P1—Co1—P3	103.72 (2)	101.61 (2)
P2—Co1—P3	105.67 (2)	170.58 (2)
P4—Co1—P1	170.63 (2)	109.47 (2)
P4—Co1—P2	101.97 (2)	105.03 (2)
P4—Co1—P3	71.28 (2)	71.194 (19)
P1—Co1—Cl1	95.27 (2)	135.91 (2)
P2—Co1—Cl1	131.45 (3)	91.89 (2)
P1—N1—P2	–	99.14 (9)
P1—N2—P2	101.71 (9)	–
P3—N1—P4	101.34 (9)	–
P3—N2—P4	–	102.23 (9)

2.3. Noncovalent interactions (NCI) analysis

Noncovalent interaction (NCI) calculations were performed with *NCIPLOT4* (Boto *et al.*, 2020), a density-based tool that maps subtle intermolecular forces. NCI analysis was carried out on the basis of promolecular approximations using the crystallographic atomic coordinates of the various metal complexes of interest. Reduced density gradient (RDG) isosurfaces were rendered in *VMD 1.9.3* (Humphrey *et al.*, 1996) and coloured according to $\mathrm{sign}(\lambda_2)\rho(\mathbf{r})$, where $\rho(\mathbf{r})$ is the electron density and λ_2 is the second eigenvalue of the Hessian matrix. Deep-blue (large negative) values pinpoint strongly attractive regions, such as classical hydrogen bonds, green zones near zero correspond to weak van der Waals contacts and red (positive) values flag steric repulsion (Boto *et al.*, 2020). The identical colour scale links the 3D isosurfaces

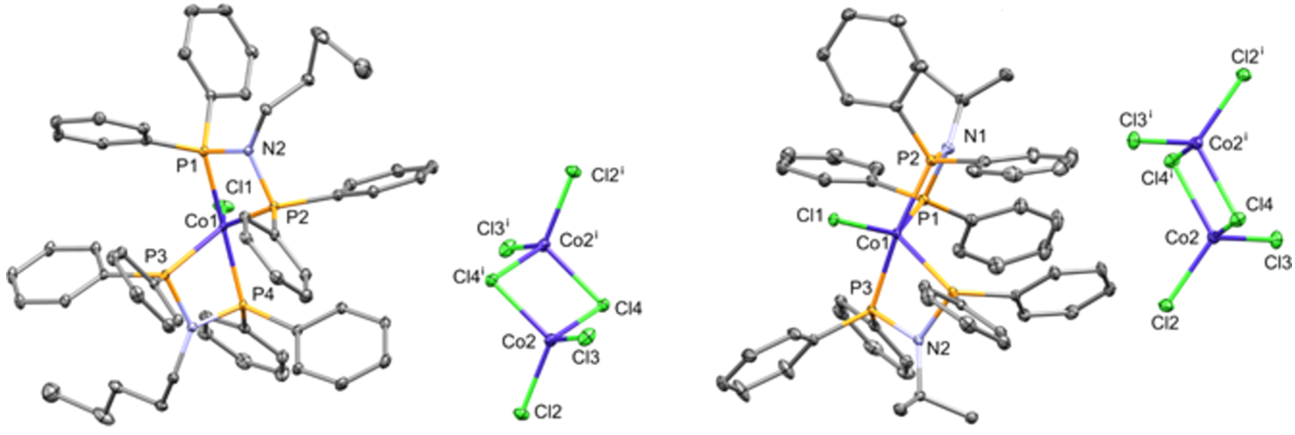

Figure 1
The molecular structures of complexes **1** (left) and **2** (right), with displacement ellipsoids drawn at the 50% probability level. All H atoms and disordered *n*-pentyl (in **1**) and isopropyl (in **2**) groups have been omitted for clarity.

Table 3
CSD survey of transition-metal complexes of the type $[TMCl_n(PNP)_2]$ (n = 1 or 2).

TBP is trigonal bipyramidal and OCT is octahedral.

CSD refcode	Geometry	Dihedral (°)	N···TM (Å)	P—N—P (°)	P···P (Å)	P—TM—P (°)	Reference
AXOSOV	TBP	77.952	2.993	100.222	2.63	69.325	Díez *et al.* (2004)
CEMTAR	OCT	4.052	3.149	103.215	2.712	66.275	Ogawa *et al.* (2013)
CEMTEV	OCT	5.091	3.138	104.698	2.729	66.354	Ogawa *et al.* (2013)
DOSWIT	OCT	1.229	2.891	103.565	2.697	72.79	Naktode *et al.* (2014)
EFARIP	OCT	8.797	3.083	105.642	2.723	66.894	Kim *et al.* (2017)
FEHZOK	OCT	6.272	2.893	102.604	2.652	71.669	Fliedel *et al.* (2016)
FEHZUQ	OCT	3.505	2.902	102.157	2.659	71.949	Fliedel *et al.* (2016)
ILIJIY	TBP	67.528	2.896	102.652	2.653	71.688	Fliedel *et al.* (2016)
ILIJOE	TBP	75.979	2.881	101.681	2.622	71.654	Fliedel *et al.* (2016)
ILIKAR	TBP	74.301	2.91	99.429	2.616	71.927	Fliedel *et al.* (2016)
FOQGAT	OCT	0	3.019	101.187	2.679	69.828	Gaw *et al.* (2000)
HUWLIU	OCT	4.387	2.974	102.386	2.641	69.256	Balakrishna *et al.* (2003)
HUWLOA	OCT	0	3.027	101.48	2.662	68.908	Balakrishna *et al.* (2003)
QAMJAQ	OCT	0	3.015	101.783	2.662	69.096	Slawin *et al.* (2004)
QIDJAQ	OCT	1.703	3.023	108.93	2.755	67.635	Stennett *et al.* (2012)
QIDJAQ	OCT	1.331	3.023	109.334	2.75	67.661	Stennett *et al.* (2012)
SESBAX	OCT	0	3.036	101.165	2.666	68.923	Naicker *et al.* (2022)
UMERUA	TBP	81.557	2.988	100.194	2.648	70.18	Aydemir *et al.* (2011)
UMESAH	OCT	0	3.01	101.518	2.663	69.392	Aydemir *et al.* (2011)
XEFXAI	TBP	66.281	3.112	107.16	2.747	66.392	Jabri *et al.* (2006)
PEHHIT	OCT	4.94	2.996	101.611	2.655	69.468	Lu *et al.* (1993)

(drawn for $-0.07 \leq$ isovalue ≤ 0.07) to the corresponding 2D NCI plots produced with *GNUPLOT 4.6* (Williams *et al.*, 2017). To gauge backbone strain, P—N—P atom sets were extracted from the CIFs of our transition-metal aminodiphosphine complexes (and analogous CSD entries) and analyzed in isolation. An analogous protocol, using the atomic coordinates of the *M*—P—N—P metallocycle, elucidated the character of the *M*···N contact within each complex.

3. Results and discussion

3.1. Description of X-ray crystal structures

Blue crystals of **1** and **2** were obtained by vapour diffusion of diethyl ether into a dichloromethane solution of the respective complexes. The molecular structures of complexes **1** and **2** are shown in Fig. 1. In both complexes, two ligands coordinate in a bidentate manner to the cobalt metal centres *via* the P atoms. Selected bond distances and angles are given in Table 2.

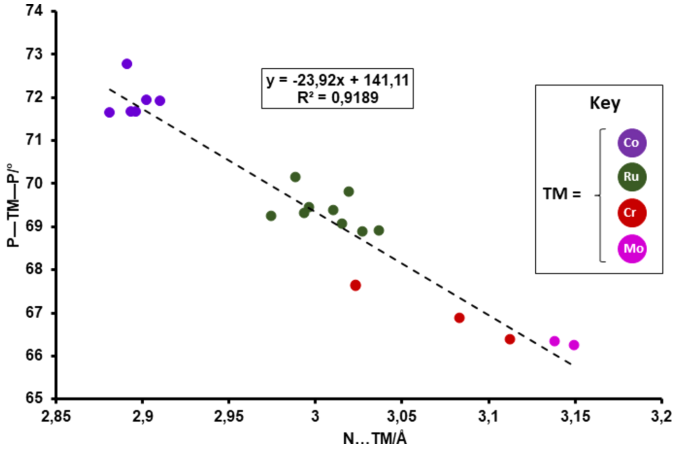

Figure 2
Correlation between the P—TM—P bite angles and N···TM contact distances in related PNP aminodiphosphine metal complexes found in the CSD.

The asymmetric unit of complex **1** contains two species: the five-coordinated cationic complex $[CoCl\{\kappa^2\text{-}P,P\text{-}(N)\text{-}C_5H_{11}\}_2]^{2+}$ and the anionic dimer $[Co_2(\mu_2\text{-}Cl)_2Cl_4]^{2-}$. The cation has a distorted trigonal-bipyramidal geometry, with the Cl atom and one P atom from each PNP ligand in the equatorial plane, and the remaining two P atoms in axial positions. In contrast, the asymmetric unit of **2** contains a molecule of the five-coordinated cation $[CoCl\{\kappa^2\text{-}P,P\text{-}(N)\text{-}C_3H_7\}_2]^{2+}$ and half of the $[Co_2(\mu_2\text{-}Cl)_2Cl_4]^{2-}$ anion. The cationic species in **2** adopts a coordination geometry similar to that of **1**.

The equatorial planes of the two complexes show P—Co—P angles of 105.67 (2) and 109.47 (2)°, and Cl—Co—P angles of 131.45 (3) and 122.88 (2)° in complex **1**, and 135.914 (18) and 114.239 (17)° in complex **2**. These angles are indicative of a distorted trigonal-pyramidal geometry. Similar geometrical distortions have been reported in other pentacoordinated transition-metal complexes with diphosphine ligands (Naktode *et al.*, 2014; Fliedel *et al.*, 2016). This was further quantified by calculating the φ (tau) index, defined as $\tau = \alpha - \beta/60$, where α and β correspond to two angles. The τ values for a perfect square-based pyramid and a perfect trigonal bipyramid are 0 and 1, respectively (Addison *et al.*, 1984). The structural distortion indices for **1** and **2** were calculated as 0.14 and 0.36, confirming the deviation from ideal geometries and the presence of intermediate distortion between square-pyramidal and trigonal-bipyramidal extremes.

The P—N—P bite angle of the bidentate ligand is acute, generating two P—N—P—Co metallacycle planes in each of the complexes, with interplanar angles between 71.58 (3) and 105.28 (4)° in both complexes, and with the Co atom displaced

slightly towards one of the P atoms. Complex **1** exhibits relatively uniform Co—P bond lengths, with equatorial bonds [2.2514 (6) and 2.2590 (6) Å] slightly shorter than the axial ones [2.2480 (6) and 2.2495 (6) Å]. In contrast, complex **2** shows greater asymmetry, with two longer Co—P distances [2.2913 (5) and 2.2654 (5) Å] and two shorter ones [2.2239 (6) and 2.2259 (6) Å], involving both equatorial and axial positions. The Co—Cl bond lengths are close in the two complexes [2.2305 (6) and 2.2398 (4) Å] and similar to the same distances in structures found in the literature.

3.2. CSD survey

A comprehensive survey of the Cambridge Structural Database (CSD, Version 5.40 with updates; Groom *et al.*, 2016) yielded 20 crystal structures of transition-metal complexes bearing bidentate aminodiphosphine (PNP) ligands with a $[TMCl_n(PNP)_2]$ core (TM = transition metal and n = 1 or 2) (Table 3). Ruthenium was the most represented (with 8), followed by cobalt(II) (7), chromium (3) and molybdenum(II) (2). Notably, the ligands feature diverse substituents on the N atom, mainly alkyl or aryl groups, with occasional heteroatom-containing functionalities. Most complexes adopt an octahedral geometry (14 out of 20), while trigonal-bipyramidal geometries are less common, occurring in only six structures. This distribution reflects the combined steric and electronic influences of the PNP ligands and the inherent preferences of the metal centres.

One key geometric observation across the dataset is an inverse correlation between the P—TM—P bite angle and the nonbonded N···TM contact distance. As can be seen in the scatter plot (Fig. 2), complexes with larger P—TM—P bite angles exhibit shorter N···TM contacts. This suggests that wider bite angles may push the N atom into closer proximity with the metal centre, despite the lack of any formal bonding. The observed trend correlates well with the van der Waals radii of the metals: smaller metals like cobalt (1.63 Å) can accommodate wider P—TM—P angles, resulting in shorter N···TM distances. In contrast, larger metals such as ruthenium (1.78 Å) and molybdenum (1.90 Å) typically exhibit narrower bite angles and longer N···TM separations. Chromium, with an intermediate radius (1.66 Å), shows values consistent with this relationship.

The nature of the metal centre significantly influences the conformation of the PNP ligand (the P···P distance in particular). A CSD study of uncoordinated PNP gave an average

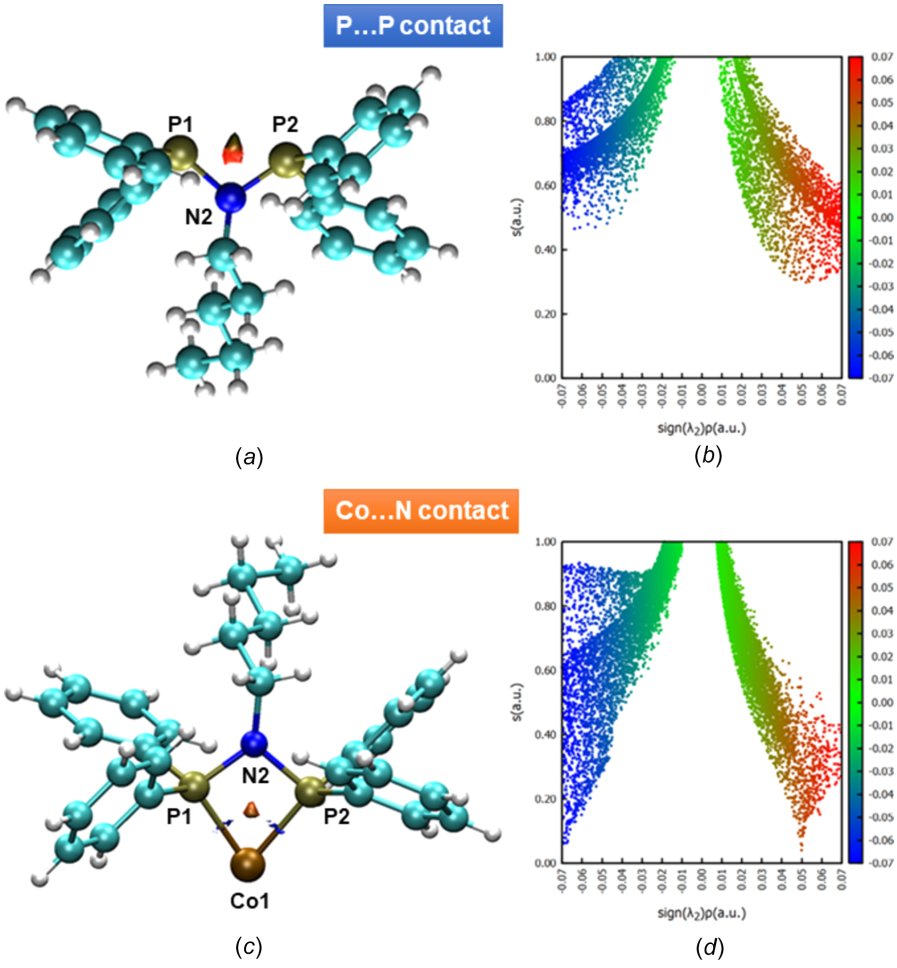

Figure 3
(*a*) 3D and (*b*) 2D representations of the NCI plots of the coordinated aminodiphosphine ligands in complex **1**. (*c*) 3D and (*d*) 2D representations of the NCI plots focusing on the Co···N contacts in complex **1**.

P···P distance of 2.988 Å (Engelbrecht *et al.*, 2011; Keat *et al.*, 1981; Dunesha *et al.*, 2016; Cotton *et al.*, 1996; Gimbert *et al.*, 1999; Tobias & Hans-Christian, 2012; Luo *et al.*, 2013; Cloete *et al.*, 2009; Liu, 2014), showing flexibility and an unconstrained backbone. On coordination, a shorter P···P distance due to chelation was observed. This chelation effect is observed in complexes **1** and **2**, which have P···P distances of 2.6248 (8)–2.6263(9) and 2.5895 (6)–2.6528 (5) Å, respectively. Similar trends were observed across the 20 related transition-metal complexes from the CSD: Cr complexes showed P···P distances ranging between 2.723 and 2.755 Å, Mo between 2.712 and 2.729 Å, Ru between 2.63 and 2.679 Å, and Co between 2.616 and 2.697 Å (Table 3). The trend suggests that smaller metal centres, such as Co (van der Waals radius $\simeq$ 1.63 Å), pull the P atoms closer together, leading to shorter P···P distances. In contrast, larger metals like Mo ($\simeq$1.90 Å) allow a more extended ligand conformation, resulting in longer P···P separations (Duncan Lyngdoh *et al.*, 2018). Additionally, P—TM bonding increases the electron-density redistribution, which strengthens the P—TM bonds and indirectly contributes to a shortening of the P···P distances (Rauch *et al.*, 2020). In complexes **1** and **2**, the steric properties of the N-substituent do not substantially alter the P···P separation [2.6248 (8)–2.6263 (9) Å in **1** and 2.5895 (6)–2.6528 (5) Å in **2**], even though they could still contribute to the overall ligand environment.

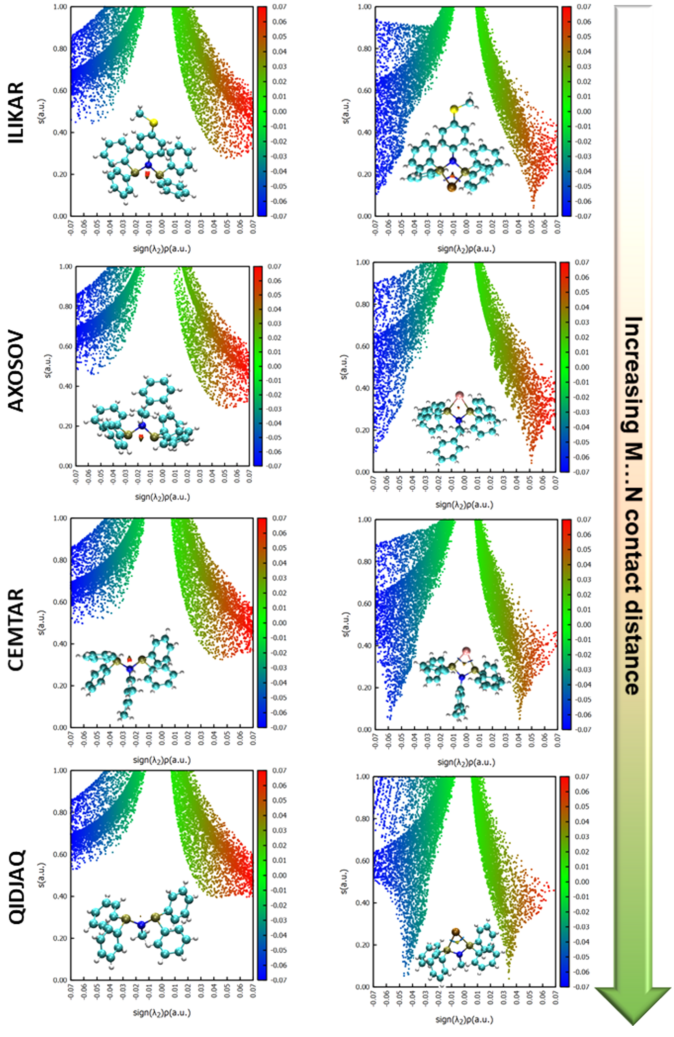

Figure 4
3D representations and corresponding 2D NCI plots for selected CSD refcodes with coordinated aminodiphosphine ligands (left) and their transition-metal complexes (right).

3.3. NCI analysis of P···P and Co···N contacts

Noncovalent interaction (NCI) analysis was conducted using the promolecular approximation, which provides a computationally efficient and qualitative description of NCI regions, but should not be relied upon for quantitative electron-density analysis. Interactions were assessed using 3D NCI plots complemented by 2D scatter plots from reduced density gradient (RDG) calculations, which are shown in Fig. 3. For the P···P contacts, distinct regions were identified by orange-coloured RDG isosurfaces in the 3D representation [Fig. 3(*a*)]. This coloration indicates relatively strong steric repulsion or destabilizing interactions, consistent with close interatomic distances significantly shorter than the sum of the P-atom van der Waals radii ($\sim$3.6 Å). These shortened distances suggest significant steric hindrance between the phosphorus centres, emphasizing repulsive interactions rather than stabilizing dispersive interactions. The 2D scatter plots support this interpretation, displaying characteristic peaks in the positive region of the electron density multiplied by the second Hessian eigenvalue, confirming the predominantly repulsive nature of these interactions.

The NCI analysis of the Co···N interaction within complex **1** also showed orange-coloured RDG isosurfaces, indicating a notable degree of steric repulsion or strain around the metal coordination site. The Co···N contacts exhibited features consistent with partially destabilizing interactions, which likely arise due to steric constraints imposed by ligand architecture or coordination geometry. Correspondingly, the 2D scatter plots revealed distinctive peaks extending into the positive region of electron density multiplied by the second Hessian eigenvalue, further substantiating the sterically dominated nature of the Co···N interactions.

The NCI analysis was extended to other [$TMCl_n(PNP)_2$] complexes according to the CSD survey in Section 3.2. Only one of each representative transition-metal type of [$TMCl_n$-$(PNP)_2$] complexes was selected for this analysis. The 3D representations and corresponding 2D scatter plots demonstrated pronounced orange-coloured isosurfaces and positive RDG peaks between the P atoms in the ligands (Fig. 4), similar to that of complex **1** [Figs. 3(*a*) and 3(*b*)], thus suggesting a repulsion rather than attractive dispersive interaction between the P atoms. Upon coordination with Co (CSD refcode ILIKAR; Fliedel *et al.*, 2016) and Ru (AXOSOV; Díez *et al.*, 2004), similar orange-coloured RDG isosurfaces persist in the *M*···N interaction zones, alongside characteristic positive peaks around the 0.05 sign(λ_2)ρ(**r**) eigenvalue in the corresponding 2D scatter plot (Fig. 4). As for the Mo (CEMTAR; Ogawa *et al.*, 2013) and Cr (QIDJAQ; Stennett *et*

al., 2012) complexes, the $M\cdots$N interaction zones also exhibited characteristic positive peaks around the 0.04 and 0.035 sign(λ_2)ρ(**r**) values, respectively, which could imply that there is a lesser degree of repulsion between the transition metal and its corresponding ligand. Interestingly, the sign(λ_2)ρ values of the Mo—P bond in CEMTAR were found to be around −0.06, which is greater than that of Co—P (ILIKAR) and Ru—P (AXOSOV), which are ≤ −0.07. This implies that the Mo—P bond has an inherently weaker attraction between the Mo and P atoms than that seen for Co—P (ILIKAR) and Ru—P (AXOSOV). Finally, looking at the Cr—P bond in QIDJAQ, we observe sign(λ_2)ρ(**r**) values between −0.05 and −0.04, which is typically in the range of hydrogen bonding (Zamisa *et al.*, 2022) or weak noncovalent interactions (Mphahlele *et al.*, 2023). This suggests that the Cr—P bond in QIDJAQ is much weaker than the other M—P bonds investigated in this work and this could be the determining factor behind elongated Cr$\cdots$N distances which ultimately leads to weaker coordination of the aminodiphosphine ligand to Cr.

4. Conclusion

Two novel cobalt complexes (**1** and **2**), each bearing a [CoCl(PNP-κ^2P,P')$_2$] core, were successfully synthesized and structurally characterized in the solid state. Both adopt distorted trigonal-bipyramidal geometries with coordination occurring exclusively through the P atoms of the PNP ligands. Complexes **1** and **2** feature five-coordinated [CoCl{κ^2-*P*,*P*-(*N*)-C_5H_{11}}$_2$]$^{2+}$ and [CoCl{κ^2-*P*,*P*-(*N*)-C_3H_7}$_2$]$^{2+}$ cationic species, respectively, along with [$Co_2(\mu_2$-Cl)$_2$Cl$_4$]$^{2-}$ counter-ions. A comprehensive CSD survey, complemented by noncovalent interaction (NCI) analysis, provided further insight into the relationship between structural features and metal identity. The survey confirmed that octahedral geometries dominate among [TMCl$_n$(PNP)$_2$] complexes, while trigonal-bipyramidal geometries are relatively rare, reflecting the steric and electronic constraints imposed by the PNP ligand framework and the preferences of individual metal centres. A key trend identified was an inverse correlation between the P—TM—P bite angles and the N$\cdots$TM contact distances, which is largely governed by the van der Waals radii of the metals. Smaller metals like cobalt (1.63 Å) accommodate wider bite angles and shorter stronger N$\cdots$TM interactions. In contrast, larger metals such as ruthenium (1.78 Å) and molybdenum (1.90 Å) exhibit narrower bite angles and longer N$\cdots$TM contacts, with chromium showing intermediate behaviour. NCI analysis revealed notable steric repulsion at Co$\cdots$N contact points, indicating strain within the coordination sphere likely induced by the constrained ligand geometry. Similar effects were observed across the broader dataset of [TMCl$_n$(PNP)$_2$] complexes. The sign(λ_2)ρ eigenvalues further suggest that Mo—P bonds are weaker than their Co—P and Ru—P counterparts, with Cr—P interactions being the weakest overall. Despite the potential for moderate-to-strong $M\cdots$N interactions, steric hindrance from the ligand backbone significantly limits such coordination. However, to obtain a more accurate representation of the electron-density distribution, NCI analysis based on quantum-chemical wavefunction is required, as it accounts for electronic relaxation, polarization and charge-transfer effects that the promolecular approximation cannot capture. These insights highlight how subtle structural and electronic factors — such as ligand bite angle, metal size and steric effects — govern coordination in PNP-ligated transition-metal complexes, offering valuable guidance for their design in catalysis and materials chemistry.

Acknowledgements

We gratefully acknowledge financial support from NRF, THRIP and UKZN (URF). Sizwe J. Zamisa contributed to the writing – original draft, conceptualization and data curation; Adesola A. Adeleke to the writing – original draft, conceptualization and data curation; Dunesha Naicker to the writing – original draft and data curation; Holger B. Friedrich to the writing – review and editing; and Bernard Omondi to the writing – review and editing.

Data availability

The authors declare no competing interests.

References

Addison, A. W., Rao, T. N., Reedijk, J., van Rijn, J. & Verschoor, G. C. (1984). *J. Chem. Soc. Dalton Trans.* pp. 1349–1356.
Aydemir, M., Baysal, A., Özkar, S. & Yıldırım, L. T. (2011). *Inorg. Chim. Acta* **367**, 166–172.
Balakrishna, M. S., Panda, R. & Mague, J. T. (2003). *Polyhedron* **22**, 587–593.
Beims, N., Greven, T., Schmidtmann, M. & van der Vlugt, J. I. (2023). *Chem. A Eur. J.* **29**, e202302463.
Blann, K., Bollmann, A., Dixon, J. T., Hess, F. M., Killian, E., Maumela, H., Morgan, D. H., Neveling, A., Otto, S. & Overett, M. J. (2005). *Chem. Commun.* pp. 620–621.
Boto, R. A., Peccati, F., Laplaza, R., Quan, C., Carbone, A., Piquemal, J.-P., Maday, Y. & Contreras-Garcı, A. J. (2020). *J. Chem. Theory Comput.* **16**, 4150–4158.
Bourhis, L. J., Dolomanov, O. V., Gildea, R. J., Howard, J. A. K. & Puschmann, H. (2015). *Acta Cryst.* A**71**, 59–75.
Bruker (2009). *COSMO*, *SAINT-Plus* and *SADABS*. Bruker AXS Inc., Madison, Wisconsin, USA.
Chirdon, D. N., Kelley, S. P., Hazari, N. & Bernskoetter, W. H. (2021). *Organometallics* **40**, 4066–4076.
Cloete, N., Visser, H. G., Roodt, A. & Gabrielli, W. F. (2009). *Acta Cryst.* E**65**, o3081.
Cotton, A. F., Kühn, F. E. & Yokochi, A. (1996). *Inorg. Chim. Acta* **252**, 251–256.
Cotton, F. A. & Hong, B. (1992). *Prog. Inorg. Chem* **40**, 179.
Díez, J., Gamasa, M. P., Gimeno, J., Rodríguez, Y. & García–Granda, S. (2004). *Eur. J. Inorg. Chem.* **2004**, 2078–2085.
Dolomanov, O. V., Bourhis, L. J., Gildea, R. J., Howard, J. A. K. & Puschmann, H. (2009). *J. Appl. Cryst.* **42**, 339–341.
Duncan Lyngdoh, R. H., Schaefer, H. F. III & King, R. B. (2018). *Chem. Rev.* **118**, 11626–11706.
Dunesha, N., Pramod, B. P. & Holger, B. F. (2016). *Z. Kristallogr. New Cryst. Struct.* **231**, 653–656.
Engelbrecht, I., Visser, H. G. & Roodt, A. (2011). *Acta Cryst.* E**67**, o2041–o2042.

Fliedel, C., Rosa, V., Vileno, B., Parizel, N., Choua, S., Gourlaouen, C., Rosa, P., Turek, P. & Braunstein, P. (2016). *Inorg. Chem.* **55**, 4183–4198.
Gaw, K. G., Smith, M. B. & Slawin, A. M. Z. (2000). *New J. Chem.* **24**, 429–435.
Gimbert, Y., Robert, F., Durif, A., Averbuch, M.-T., Kann, N. & Greene, A. E. (1999). *J. Org. Chem.* **64**, 3492–3497.
Groom, C. R., Bruno, I. J., Lightfoot, M. P. & Ward, S. C. (2016). *Struct. Sci.* **72**, 171–179.
Hierso, J.-C., Amardeil, R., Bentabet, E., Broussier, R., Gautheron, B., Meunier, P. & Kalck, P. (2003). *Coord. Chem. Rev.* **236**, 143–206.
Humphrey, W., Dalke, A. & Schulten, K. (1996). *J. Mol. Graph.* **14**, 33–38.
Jabri, A., Crewdson, P., Gambarotta, S., Korobkov, I. & Duchateau, R. (2006). *Organometallics* **25**, 715–718.
Keat, R., Manojlović-Muir, L., Muir, K. W. & Rycroft, D. S. (1981). *J. Chem. Soc. Dalton Trans.* pp. 2192–2198.
Kim, E. H., Lee, H. M., Jeong, M. S., Ryu, J. Y., Lee, J. & Lee, B. Y. (2017). *ACS Omega* **2**, 765–773.
Konrath, R., Spannenberg, A. & Kamer, P. (2019). *Chem. A Eur. J.* **25**, 15341–15350.
Liu, X.-F. (2014). *Inorg. Chim. Acta* **421**, 10–17.
Lu, Y. Z. Z.-Z., Zhao, W.-J., Wang, H.-G. & Ma, Y.-F. (1993). *Jiegou Huaxue (Chin.) (Chin. J. Struct. Chem.)* **12**, 129.
Luo, L.-J., Liu, X.-F. & Gao, H.-Q. (2013). *J. Coord. Chem.* **66**, 1077–1083.
Mayer, H. A. & Kaska, W. C. (1994). *Chem. Rev.* **94**, 1239–1272.
Mphahlele, M. J., El-Gogary, T. M. & Zamisa, S. J. (2023). *J. Mol. Struct.* **1294**, 136501.
Munzeiwa, W. A., Omondi, B. & Nyamori, V. O. (2020). *Beilstein J. Org. Chem.* **16**, 362–383.
Naicker, D., Alapour, S., Zamisa, S. J. & Friedrich, H. B. (2022). *J. Coord. Chem.* **75**, 1129–1146.
Naicker, D., Friedrich, H. B. & Omondi, B. (2015). *RSC Adv.* **5**, 63123–63129.
Naktode, K., Kottalanka, R. K., Adimulam, H. & Panda, T. K. (2014). *J. Coord. Chem.* **67**, 3042–3053.
Ogawa, T., Kajita, Y., Wasada-Tsutsui, Y., Wasada, H. & Masuda, H. (2013). *Inorg. Chem.* **52**, 182–195.
Olding, A., Lucas, N. T., Ho, C. C. & Bissember, A. C. (2024). *Dalton Trans.* **53**, 4471–4478.
Overett, M. J., Blann, K., Bollmann, A., Dixon, J. T., Hess, F., Killian, E., Maumela, H., Morgan, D. H., Neveling, A. & Otto, S. (2005). *Chem. Commun.* pp. 622–624.
Rauch, M., Kar, S., Kumar, A., Avram, L., Shimon, L. J. W. & Milstein, D. (2020). *J. Am. Chem. Soc.* **142**, 14513–14521.
Sheldrick, G. M. (2008). *Acta Cryst.* A**64**, 112–122.
Slawin, A. M. Z., Milton, H. L., Wheatley, J. & Woollins, J. D. (2004). *Polyhedron* **23**, 3125–3132.
Smith, M. B. (2022). *Molecules* **27**, 6293.
Spek, A. L. (2020). *Acta Cryst.* E**76**, 1–11.
Stennett, T. E., Haddow, M. F. & Wass, D. F. (2012). *Organometallics* **31**, 6960–6965.
Tobias, M. & Hans-Christian, B. (2012). *Z. Naturforsch. B* **67**, 504–506.
Vasilenko, V., Roth, T., Blasius, C. K., Intorp, S. N., Wadepohl, H. & Gade, L. H. (2016). *Beilstein J. Org. Chem.* **12**, 846–853.
Williams, T., Kelley, C., Bröker, H., Campbell, J., Cunningham, R., Denholm, D., Elber, E., Fearick, R., Grammes, C. & Hart, L. (2017). *GNUPLOT 4.6*. http://www.gnuplot.info/.
Zamisa, S. J., Ngubane, N. P., Adeleke, A. A., Jonnalagadda, S. B. & Omondi, B. (2022). *Cryst. Growth Des.* **22**, 5814–5834.
Zhao, P.-H., Ma, Z.-Y., Hu, M.-Y., He, J., Wang, Y.-Z., Jing, X.-B., Chen, H.-Y., Wang, Z. & Li, Y.-L. (2018). *Organometallics* **37**, 1280–1290.

supporting information

Acta Cryst. (2025). C**81**, 694-701 [https://doi.org/10.1107/S2053229625009519]

Structural insights into transition-metal–aminodiphosphine (PNP) complexes bearing [$MCl_n(PNP)_2$] (M = Co, Ru, Cr or Mo; n = 1 or 2) cores in the solid state

Sizwe J. Zamisa, Adesola A. Adeleke, Dunesha Naicker, Holger B. Friedrich and Bernard Omondi

Computing details

Bis[bis(diphenylphosphanyl)(pentyl)amine-κ^2P,P']chloridocobalt(III) di-μ-chlorido-bis[dichloridocobalt(II)] (1)

Crystal data

$[CoCl(C_{29}H_{31}NP_2)_2][Co_2Cl_6]$
M_r = 1336.01
Triclinic, $P\overline{1}$
a = 11.5114 (4) Å
b = 12.6404 (4) Å
c = 20.7858 (7) Å
α = 89.481 (2)°
β = 82.999 (2)°
γ = 68.324 (2)°
V = 2787.57 (17) Å^3
Z = 2
$F(000)$ = 1215.952
D_x = 1.592 Mg m^{-3}
Mo $K\alpha$ radiation, λ = 0.71073 Å
Cell parameters from 9866 reflections
θ = 2.2–28.2°
μ = 1.38 mm^{-1}
T = 100 K
Block, green
0.35 × 0.22 × 0.14 mm

Data collection

Bruker SMART APEXII area detector diffractometer
Detector resolution: 7.9 pixels mm^{-1}
ω and φ scans
Absorption correction: multi-scan (SADABS; Bruker, 2009)
T_{min} = 0.640, T_{max} = 0.746
74041 measured reflections
13808 independent reflections
11199 reflections with $I \geq 2u(I)$
R_{int} = 0.042
θ_{max} = 28.3°, θ_{min} = 1.7°
h = −15→15
k = −16→16
l = −27→27

Refinement

Refinement on F^2
Least-squares matrix: full
$R[F^2 > 2\sigma(F^2)]$ = 0.040
$wR(F^2)$ = 0.113
S = 1.06
13808 reflections
691 parameters
242 restraints
134 constraints
Primary atom site location: structure-invariant direct methods
H-atom parameters constrained
$w = 1/[\sigma^2(F_o^2) + (0.0606P)^2 + 2.4052P]$ where $P = (F_o^2 + 2F_c^2)/3$
$(\Delta/\sigma)_{max}$ = 0.0001
$\Delta\rho_{max}$ = 1.13 e Å^{-3}
$\Delta\rho_{min}$ = −0.62 e Å^{-3}

Special details

Refinement. Crystals of the complexes were each selected and glued onto the tip of glass fibers. The crystals were then mounted in a stream of cold nitrogen at 100 (1) K and centred in the X-ray beam using a video camera. Crystal evaluation and data collection were performed on a Bruker SMART APEXII diffractometer with Mo K_α radiation (λ = 0.71073 Å) and a diffractometer-to-crystal distance of 4.00 cm. The initial cell matrix was obtained from three series of scans at different starting angles. Each series consisted of 12 frames collected at intervals of 0.5° in a 6° range with the exposure time of about 10 s per frame. The reflections were indexed successfully by an automated indexing routine built in the APEX2 program suite (Bruker, 2009). Data collection method involved ω scans of width 0.5°. Data reduction was carried out using SAINT-Plus (Bruker, 2009). The structures were solved by direct methods using SHELXS (Sheldrick, 2008) and refined using olex2.refine (Dolomanov et al., 2009). Both structures were checked for solvent-accessible cavities using PLATON (Spek, 2020) and the graphics were created with OLEX2 (Dolomanov et al., 2009). Non-H atoms were first refined isotropically and then by anisotropic refinement with full-matrix least-squares calculations based on F^2 using SHELXS.

Fractional atomic coordinates and isotropic or equivalent isotropic displacement parameters (Å²)

	x	*y*	*z*	U_{iso}*/U_{eq}	Occ. (<1)
Co1	0.47226 (2)	0.27095 (2)	0.195882 (13)	0.01252 (7)	
Cl1	0.40827 (6)	0.24946 (5)	0.10150 (3)	0.03051 (14)	
P1	0.66671 (5)	0.13715 (4)	0.17250 (3)	0.01369 (11)	
P2	0.51485 (5)	0.15629 (4)	0.28044 (3)	0.01335 (11)	
P3	0.50833 (5)	0.42752 (4)	0.22346 (2)	0.01248 (11)	
P4	0.28768 (5)	0.40751 (4)	0.23513 (3)	0.01327 (11)	
N1	0.35207 (16)	0.50547 (15)	0.24549 (9)	0.0146 (3)	
N2	0.65936 (16)	0.07226 (15)	0.24316 (8)	0.0147 (3)	
C1	0.1657 (2)	0.46679 (18)	0.18224 (11)	0.0169 (4)	
C2	0.0401 (2)	0.4830 (2)	0.20108 (12)	0.0240 (5)	
H2	0.0149 (2)	0.4634 (2)	0.24329 (12)	0.0288 (6)*	
C3	−0.0488 (2)	0.5276 (2)	0.15854 (14)	0.0322 (6)	
H3	−0.1344 (2)	0.5380 (2)	0.17175 (14)	0.0386 (7)*	
C4	−0.0133 (2)	0.5569 (2)	0.09714 (13)	0.0298 (5)	
H4	−0.0744 (2)	0.5872 (2)	0.06822 (13)	0.0357 (7)*	
C5	0.1113 (2)	0.5422 (2)	0.07775 (12)	0.0260 (5)	
H5	0.1354 (2)	0.5634 (2)	0.03576 (12)	0.0312 (6)*	
C6	0.2012 (2)	0.49633 (19)	0.11975 (11)	0.0196 (4)	
H6	0.2869 (2)	0.48498 (19)	0.10605 (11)	0.0235 (5)*	
C7	0.20252 (19)	0.38601 (18)	0.31034 (10)	0.0163 (4)	
C8	0.1661 (2)	0.29199 (19)	0.31106 (11)	0.0185 (4)	
H8	0.1831 (2)	0.24577 (19)	0.27266 (11)	0.0222 (5)*	
C9	0.1054 (2)	0.2652 (2)	0.36717 (12)	0.0219 (5)	
H9	0.0816 (2)	0.2008 (2)	0.36713 (12)	0.0263 (6)*	
C10	0.0796 (2)	0.3329 (2)	0.42324 (12)	0.0254 (5)	
H10	0.0381 (2)	0.3151 (2)	0.46174 (12)	0.0305 (6)*	
C11	0.1149 (2)	0.4270 (2)	0.42282 (12)	0.0259 (5)	
H11	0.0970 (2)	0.4734 (2)	0.46122 (12)	0.0311 (6)*	
C12	0.1761 (2)	0.4540 (2)	0.36691 (11)	0.0219 (5)	
H12	0.1998 (2)	0.5184 (2)	0.36718 (11)	0.0263 (6)*	
C13	0.56244 (18)	0.50572 (17)	0.16019 (10)	0.0146 (4)	
C14	0.5656 (2)	0.47391 (19)	0.09544 (10)	0.0176 (4)	

H14	0.5436 (2)	0.41109 (19)	0.08545 (10)	0.0212 (5)*
C15	0.6011 (2)	0.5346 (2)	0.04585 (11)	0.0215 (5)
H15	0.6042 (2)	0.5124 (2)	0.00193 (11)	0.0258 (5)*
C16	0.6319 (2)	0.6268 (2)	0.05993 (12)	0.0236 (5)
H16	0.6556 (2)	0.6680 (2)	0.02572 (12)	0.0284 (6)*
C17	0.6284 (2)	0.6593 (2)	0.12403 (11)	0.0215 (5)
H17	0.6493 (2)	0.7230 (2)	0.13363 (11)	0.0258 (5)*
C18	0.5943 (2)	0.59869 (18)	0.17411 (11)	0.0178 (4)
H18	0.5928 (2)	0.62055 (18)	0.21791 (11)	0.0214 (5)*
C19	0.5890 (2)	0.44273 (17)	0.29016 (10)	0.0150 (4)
C20	0.5245 (2)	0.48039 (18)	0.35210 (11)	0.0185 (4)
H20	0.4359 (2)	0.49948 (18)	0.35985 (11)	0.0222 (5)*
C21	0.5898 (2)	0.4899 (2)	0.40238 (11)	0.0240 (5)
H21	0.5453 (2)	0.5172 (2)	0.44417 (11)	0.0288 (6)*
C22	0.7194 (3)	0.4600 (2)	0.39198 (12)	0.0269 (5)
H22	0.7635 (3)	0.4658 (2)	0.42671 (12)	0.0323 (6)*
C23	0.7846 (2)	0.4215 (2)	0.33080 (12)	0.0239 (5)
H23	0.8735 (2)	0.4009 (2)	0.32369 (12)	0.0287 (6)*
C24	0.7201 (2)	0.41305 (19)	0.27991 (11)	0.0188 (4)
H24	0.7650 (2)	0.38709 (19)	0.23803 (11)	0.0226 (5)*
C25	0.80436 (19)	0.17630 (18)	0.16508 (10)	0.0152 (4)
C26	0.8244 (2)	0.24050 (19)	0.11254 (11)	0.0183 (4)
H26	0.7659 (2)	0.26374 (19)	0.08186 (11)	0.0220 (5)*
C27	0.9299 (2)	0.2701 (2)	0.10538 (12)	0.0242 (5)
H27	0.9421 (2)	0.3150 (2)	0.07019 (12)	0.0291 (6)*
C28	1.0178 (2)	0.2349 (2)	0.14914 (12)	0.0252 (5)
H28	1.0908 (2)	0.2540 (2)	0.14342 (12)	0.0302 (6)*
C29	0.9980 (2)	0.1716 (2)	0.20113 (12)	0.0230 (5)
H29	1.0579 (2)	0.1470 (2)	0.23110 (12)	0.0276 (6)*
C30	0.8909 (2)	0.14392 (19)	0.20977 (11)	0.0190 (4)
H30	0.8768 (2)	0.10267 (19)	0.24637 (11)	0.0228 (5)*
C31	0.7099 (2)	0.02686 (18)	0.10850 (10)	0.0168 (4)
C32	0.6181 (2)	−0.00756 (19)	0.08767 (11)	0.0198 (4)
H32	0.5327 (2)	0.02783 (19)	0.10639 (11)	0.0237 (5)*
C33	0.6504 (2)	−0.09303 (19)	0.03983 (12)	0.0227 (5)
H33	0.5870 (2)	−0.11469 (19)	0.02529 (12)	0.0272 (6)*
C34	0.7753 (2)	−0.1469 (2)	0.01320 (12)	0.0269 (5)
H34	0.7972 (2)	−0.2048 (2)	−0.01986 (12)	0.0322 (6)*
C35	0.8679 (2)	−0.1159 (2)	0.03497 (13)	0.0303 (6)
H35	0.9537 (2)	−0.1545 (2)	0.01781 (13)	0.0364 (7)*
C36	0.8356 (2)	−0.0285 (2)	0.08189 (12)	0.0232 (5)
H36	0.8992 (2)	−0.0064 (2)	0.09584 (12)	0.0278 (6)*
C37	0.5389 (2)	0.19656 (18)	0.35963 (10)	0.0164 (4)
C38	0.6588 (2)	0.18773 (18)	0.37207 (11)	0.0185 (4)
H38	0.7278 (2)	0.16206 (18)	0.33843 (11)	0.0222 (5)*
C39	0.6777 (2)	0.21607 (19)	0.43291 (11)	0.0217 (5)
H39	0.7598 (2)	0.20793 (19)	0.44137 (11)	0.0260 (5)*
C40	0.5763 (2)	0.2566 (2)	0.48176 (11)	0.0245 (5)

H40	0.5892 (2)	0.2766 (2)	0.52351 (11)	0.0294 (6)*	
C41	0.4563 (2)	0.2678 (2)	0.46977 (11)	0.0250 (5)	
H41	0.3871 (2)	0.2965 (2)	0.50314 (11)	0.0300 (6)*	
C42	0.4372 (2)	0.23722 (19)	0.40909 (11)	0.0203 (4)	
H42	0.3553 (2)	0.24385 (19)	0.40111 (11)	0.0243 (5)*	
C43	0.4309 (2)	0.06083 (18)	0.29741 (11)	0.0174 (4)	
C44	0.3716 (2)	0.03644 (19)	0.24784 (12)	0.0218 (5)	
H44	0.3689 (2)	0.07528 (19)	0.20838 (12)	0.0261 (5)*	
C45	0.3167 (2)	−0.0449 (2)	0.25640 (14)	0.0291 (5)	
H45	0.2756 (2)	−0.0610 (2)	0.22296 (14)	0.0350 (7)*	
C46	0.3219 (2)	−0.1024 (2)	0.31386 (15)	0.0329 (6)	
H46	0.2851 (2)	−0.1584 (2)	0.31936 (15)	0.0394 (7)*	
C47	0.3802 (2)	−0.0790 (2)	0.36295 (13)	0.0285 (5)	
H47	0.3833 (2)	−0.1187 (2)	0.40210 (13)	0.0342 (7)*	
C48	0.4346 (2)	0.00301 (19)	0.35525 (12)	0.0224 (5)	
H48	0.4741 (2)	0.01957 (19)	0.38927 (12)	0.0269 (6)*	
C49	0.2949 (2)	0.62757 (18)	0.26781 (11)	0.0186 (4)	
H49a	0.3638 (2)	0.65559 (18)	0.27087 (11)	0.0224 (5)*	
H49b	0.2499 (2)	0.63241 (18)	0.31208 (11)	0.0224 (5)*	
C50	0.2034 (2)	0.70725 (19)	0.22553 (12)	0.0224 (5)	
H50a	0.1409 (2)	0.67395 (19)	0.21719 (12)	0.0269 (6)*	
H50b	0.1572 (2)	0.78079 (19)	0.24984 (12)	0.0269 (6)*	
C51	0.2655 (2)	0.7301 (2)	0.16081 (12)	0.0255 (5)	
H51a	0.3297 (2)	0.7620 (2)	0.16781 (12)	0.0306 (6)*	
H51b	0.3072 (2)	0.6584 (2)	0.13418 (12)	0.0306 (6)*	
C52A	0.1857 (16)	0.8131 (12)	0.1143 (8)	0.031 (2)	0.45 (3)
H52a	0.1243 (16)	0.7826 (12)	0.1007 (8)	0.038 (2)*	0.45 (3)
H52b	0.1374 (16)	0.8869 (12)	0.1380 (8)	0.038 (2)*	0.45 (3)
C53A	0.263 (2)	0.8336 (11)	0.0538 (6)	0.050 (3)	0.45 (3)
H53a	0.312 (5)	0.7608 (13)	0.0303 (17)	0.074 (4)*	0.45 (3)
H53b	0.206 (2)	0.885 (4)	0.0257 (16)	0.074 (4)*	0.45 (3)
H53c	0.321 (5)	0.868 (5)	0.0667 (6)	0.074 (4)*	0.45 (3)
C52B	0.1616 (13)	0.8152 (10)	0.1265 (7)	0.0327 (18)	0.55 (3)
H52c	0.0966 (13)	0.7835 (10)	0.1208 (7)	0.039 (2)*	0.55 (3)
H52d	0.1209 (13)	0.8868 (10)	0.1533 (7)	0.039 (2)*	0.55 (3)
C53B	0.2176 (16)	0.8399 (9)	0.0610 (5)	0.049 (2)	0.55 (3)
H53d	0.268 (4)	0.7679 (9)	0.0370 (12)	0.074 (3)*	0.55 (3)
H53e	0.1496 (16)	0.885 (4)	0.0364 (12)	0.074 (3)*	0.55 (3)
H53f	0.271 (4)	0.883 (4)	0.0671 (5)	0.074 (3)*	0.55 (3)
C54	0.7474 (2)	−0.03769 (18)	0.26340 (11)	0.0192 (4)	
H54a	0.8332 (2)	−0.04888 (18)	0.24229 (11)	0.0230 (5)*	
H54b	0.7482 (2)	−0.03191 (18)	0.31080 (11)	0.0230 (5)*	
C55A	0.709 (2)	−0.1402 (15)	0.2544 (13)	0.0194 (19)	0.366 (7)
H55a	0.638 (2)	−0.1353 (15)	0.2876 (13)	0.023 (2)*	0.366 (7)
H55b	0.681 (2)	−0.1387 (15)	0.2112 (13)	0.023 (2)*	0.366 (7)
C56A	0.8199 (8)	−0.2523 (6)	0.2602 (5)	0.0276 (17)	0.366 (7)
H56a	0.7906 (8)	−0.3159 (6)	0.2557 (5)	0.033 (2)*	0.366 (7)
H56b	0.8863 (8)	−0.2601 (6)	0.2235 (5)	0.033 (2)*	0.366 (7)

C57A	0.8787 (7)	−0.2651 (6)	0.3227 (4)	0.0333 (18)	0.366 (7)
H57a	0.9467 (7)	−0.3412 (6)	0.3219 (4)	0.040 (2)*	0.366 (7)
H57b	0.9175 (7)	−0.2074 (6)	0.3250 (4)	0.040 (2)*	0.366 (7)
C58A	0.7860 (11)	−0.2516 (10)	0.3826 (5)	0.046 (2)	0.366 (7)
H58a	0.724 (4)	−0.1732 (19)	0.387 (2)	0.069 (3)*	0.366 (7)
H58b	0.742 (5)	−0.304 (5)	0.3791 (17)	0.069 (3)*	0.366 (7)
H58c	0.8309 (13)	−0.269 (6)	0.4208 (7)	0.069 (3)*	0.366 (7)
C55B	0.7207 (12)	−0.1427 (9)	0.2486 (7)	0.0209 (14)	0.634 (7)
H55c	0.6302 (12)	−0.1280 (9)	0.2611 (7)	0.0251 (17)*	0.634 (7)
H55d	0.7415 (12)	−0.1625 (9)	0.2015 (7)	0.0251 (17)*	0.634 (7)
C56B	0.8021 (5)	−0.2429 (4)	0.2874 (3)	0.0281 (10)	0.634 (7)
H56c	0.8007 (5)	−0.3148 (4)	0.2697 (3)	0.0338 (12)*	0.634 (7)
H56d	0.8903 (5)	−0.2472 (4)	0.2800 (3)	0.0338 (12)*	0.634 (7)
C57B	0.7612 (5)	−0.2352 (5)	0.3600 (3)	0.0365 (12)	0.634 (7)
H57c	0.7461 (5)	−0.1578 (5)	0.3771 (3)	0.0438 (14)*	0.634 (7)
H57d	0.6812 (5)	−0.2483 (5)	0.3685 (3)	0.0438 (14)*	0.634 (7)
C58B	0.8614 (5)	−0.3229 (4)	0.3947 (3)	0.0411 (13)	0.634 (7)
H58d	0.874 (2)	−0.3997 (4)	0.3793 (13)	0.0616 (19)*	0.634 (7)
H58e	0.9410 (10)	−0.311 (2)	0.3857 (15)	0.0616 (19)*	0.634 (7)
H58f	0.8340 (16)	−0.315 (2)	0.4416 (3)	0.0616 (19)*	0.634 (7)
Co2	−0.04762 (3)	0.08215 (3)	0.562903 (15)	0.02027 (8)	
Cl2	−0.16452 (6)	0.26919 (5)	0.56315 (3)	0.02629 (13)	
Cl3	0.00034 (6)	0.01533 (6)	0.65979 (3)	0.03300 (15)	
Cl4	−0.13058 (5)	−0.03519 (5)	0.51348 (3)	0.02394 (12)	

Atomic displacement parameters (Å²)

	U^{11}	U^{22}	U^{33}	U^{12}	U^{13}	U^{23}
Co1	0.01491 (13)	0.01406 (13)	0.00912 (13)	−0.00623 (11)	−0.00086 (10)	0.00182 (10)
Cl1	0.0375 (3)	0.0249 (3)	0.0205 (3)	0.0022 (2)	−0.0156 (2)	−0.0059 (2)
P1	0.0158 (2)	0.0146 (2)	0.0104 (2)	−0.0059 (2)	−0.00022 (18)	0.00087 (19)
P2	0.0156 (2)	0.0142 (2)	0.0104 (2)	−0.0061 (2)	−0.00073 (18)	0.00251 (19)
P3	0.0145 (2)	0.0138 (2)	0.0095 (2)	−0.00601 (19)	−0.00055 (18)	0.00222 (18)
P4	0.0143 (2)	0.0150 (2)	0.0110 (2)	−0.00634 (19)	−0.00050 (18)	0.00154 (19)
N1	0.0121 (8)	0.0142 (8)	0.0159 (9)	−0.0040 (6)	0.0010 (6)	0.0008 (7)
N2	0.0162 (8)	0.0141 (8)	0.0115 (8)	−0.0039 (7)	0.0008 (6)	0.0025 (6)
C1	0.0181 (10)	0.0142 (9)	0.0176 (10)	−0.0045 (8)	−0.0037 (8)	0.0020 (8)
C2	0.0205 (11)	0.0271 (12)	0.0257 (12)	−0.0103 (9)	−0.0035 (9)	0.0074 (10)
C3	0.0189 (11)	0.0344 (14)	0.0446 (16)	−0.0094 (10)	−0.0116 (11)	0.0124 (12)
C4	0.0288 (13)	0.0297 (13)	0.0327 (14)	−0.0090 (10)	−0.0177 (11)	0.0100 (11)
C5	0.0277 (12)	0.0265 (12)	0.0209 (12)	−0.0053 (10)	−0.0079 (9)	0.0057 (9)
C6	0.0189 (10)	0.0201 (10)	0.0185 (11)	−0.0053 (8)	−0.0034 (8)	0.0011 (8)
C7	0.0157 (9)	0.0190 (10)	0.0128 (10)	−0.0054 (8)	−0.0001 (7)	0.0029 (8)
C8	0.0173 (10)	0.0193 (10)	0.0189 (11)	−0.0070 (8)	−0.0020 (8)	0.0034 (8)
C9	0.0187 (10)	0.0229 (11)	0.0259 (12)	−0.0103 (9)	−0.0021 (9)	0.0091 (9)
C10	0.0225 (11)	0.0311 (12)	0.0204 (12)	−0.0096 (10)	0.0039 (9)	0.0085 (10)
C11	0.0300 (12)	0.0277 (12)	0.0163 (11)	−0.0092 (10)	0.0057 (9)	−0.0003 (9)
C12	0.0258 (11)	0.0218 (11)	0.0166 (11)	−0.0093 (9)	0.0048 (9)	−0.0002 (9)

C13	0.0135 (9)	0.0161 (9)	0.0132 (10)	−0.0051 (8)	0.0001 (7)	0.0037 (7)
C14	0.0192 (10)	0.0203 (10)	0.0151 (10)	−0.0094 (8)	−0.0022 (8)	0.0026 (8)
C15	0.0230 (11)	0.0303 (12)	0.0136 (10)	−0.0129 (9)	−0.0020 (8)	0.0060 (9)
C16	0.0255 (11)	0.0312 (12)	0.0194 (11)	−0.0161 (10)	−0.0054 (9)	0.0133 (9)
C17	0.0251 (11)	0.0224 (11)	0.0227 (12)	−0.0147 (9)	−0.0058 (9)	0.0075 (9)
C18	0.0184 (10)	0.0203 (10)	0.0157 (10)	−0.0079 (8)	−0.0038 (8)	0.0052 (8)
C19	0.0204 (10)	0.0148 (9)	0.0121 (10)	−0.0089 (8)	−0.0030 (8)	0.0033 (7)
C20	0.0215 (10)	0.0189 (10)	0.0151 (10)	−0.0080 (8)	−0.0006 (8)	0.0036 (8)
C21	0.0354 (13)	0.0246 (11)	0.0132 (11)	−0.0127 (10)	−0.0026 (9)	0.0016 (9)
C22	0.0389 (14)	0.0309 (13)	0.0179 (12)	−0.0186 (11)	−0.0122 (10)	0.0054 (10)
C23	0.0229 (11)	0.0288 (12)	0.0232 (12)	−0.0121 (10)	−0.0073 (9)	0.0074 (10)
C24	0.0208 (10)	0.0192 (10)	0.0170 (11)	−0.0083 (8)	−0.0019 (8)	0.0031 (8)
C25	0.0152 (9)	0.0158 (9)	0.0134 (10)	−0.0050 (8)	0.0009 (7)	−0.0011 (8)
C26	0.0207 (10)	0.0198 (10)	0.0144 (10)	−0.0081 (8)	0.0003 (8)	−0.0002 (8)
C27	0.0282 (12)	0.0260 (12)	0.0201 (11)	−0.0149 (10)	0.0059 (9)	0.0014 (9)
C28	0.0221 (11)	0.0284 (12)	0.0271 (13)	−0.0137 (10)	0.0036 (9)	−0.0033 (10)
C29	0.0205 (11)	0.0248 (11)	0.0247 (12)	−0.0090 (9)	−0.0043 (9)	−0.0014 (9)
C30	0.0209 (10)	0.0201 (10)	0.0165 (10)	−0.0084 (8)	−0.0017 (8)	0.0001 (8)
C31	0.0218 (10)	0.0149 (9)	0.0115 (10)	−0.0049 (8)	−0.0004 (8)	0.0027 (7)
C32	0.0221 (10)	0.0179 (10)	0.0180 (11)	−0.0063 (8)	−0.0016 (8)	0.0018 (8)
C33	0.0290 (12)	0.0182 (10)	0.0223 (12)	−0.0099 (9)	−0.0053 (9)	0.0021 (9)
C34	0.0372 (13)	0.0200 (11)	0.0208 (12)	−0.0091 (10)	0.0015 (10)	−0.0055 (9)
C35	0.0262 (12)	0.0286 (13)	0.0309 (14)	−0.0066 (10)	0.0049 (10)	−0.0098 (11)
C36	0.0223 (11)	0.0239 (11)	0.0223 (12)	−0.0078 (9)	−0.0012 (9)	−0.0020 (9)
C37	0.0224 (10)	0.0164 (10)	0.0109 (10)	−0.0076 (8)	−0.0025 (8)	0.0045 (8)
C38	0.0218 (10)	0.0184 (10)	0.0157 (10)	−0.0079 (8)	−0.0027 (8)	0.0030 (8)
C39	0.0278 (11)	0.0192 (10)	0.0184 (11)	−0.0076 (9)	−0.0085 (9)	0.0045 (8)
C40	0.0369 (13)	0.0220 (11)	0.0144 (11)	−0.0098 (10)	−0.0067 (9)	0.0037 (9)
C41	0.0310 (12)	0.0259 (12)	0.0149 (11)	−0.0084 (10)	0.0017 (9)	0.0015 (9)
C42	0.0222 (11)	0.0222 (11)	0.0156 (11)	−0.0078 (9)	−0.0004 (8)	0.0035 (8)
C43	0.0165 (9)	0.0147 (9)	0.0202 (11)	−0.0060 (8)	0.0007 (8)	0.0010 (8)
C44	0.0199 (10)	0.0199 (10)	0.0243 (12)	−0.0069 (9)	0.0005 (9)	−0.0008 (9)
C45	0.0234 (11)	0.0243 (12)	0.0416 (15)	−0.0114 (10)	−0.0024 (10)	−0.0069 (11)
C46	0.0263 (12)	0.0204 (12)	0.0520 (17)	−0.0129 (10)	0.0085 (11)	−0.0022 (11)
C47	0.0288 (12)	0.0190 (11)	0.0346 (14)	−0.0091 (10)	0.0085 (10)	0.0053 (10)
C48	0.0228 (11)	0.0178 (10)	0.0243 (12)	−0.0070 (9)	0.0036 (9)	0.0035 (9)
C49	0.0236 (10)	0.0159 (10)	0.0155 (10)	−0.0075 (8)	0.0016 (8)	−0.0008 (8)
C50	0.0207 (11)	0.0162 (10)	0.0284 (12)	−0.0042 (8)	−0.0037 (9)	−0.0005 (9)
C51	0.0322 (12)	0.0189 (10)	0.0239 (12)	−0.0067 (9)	−0.0073 (9)	0.0062 (8)
C52A	0.040 (3)	0.024 (3)	0.026 (3)	−0.005 (2)	−0.011 (2)	0.0094 (19)
C53A	0.054 (6)	0.053 (5)	0.033 (3)	−0.010 (4)	−0.007 (3)	0.024 (2)
C52B	0.040 (3)	0.027 (3)	0.026 (4)	−0.0056 (19)	−0.011 (2)	0.0099 (19)
C53B	0.046 (5)	0.059 (4)	0.035 (3)	−0.009 (3)	−0.011 (3)	0.025 (2)
C54	0.0200 (10)	0.0156 (9)	0.0205 (11)	−0.0047 (7)	−0.0034 (8)	0.0043 (7)
C55A	0.022 (3)	0.015 (2)	0.019 (3)	−0.0058 (12)	−0.0006 (17)	0.0019 (12)
C56A	0.029 (3)	0.016 (2)	0.036 (4)	−0.0057 (15)	−0.0056 (19)	0.0055 (15)
C57A	0.039 (3)	0.023 (3)	0.038 (3)	−0.0087 (19)	−0.0120 (18)	0.0093 (17)
C58A	0.054 (5)	0.047 (5)	0.039 (4)	−0.020 (3)	−0.006 (2)	0.007 (2)

C55B	0.023 (2)	0.0186 (18)	0.020 (3)	−0.0070 (11)	−0.0001 (17)	0.0012 (10)
C56B	0.032 (2)	0.0182 (17)	0.033 (2)	−0.0077 (12)	−0.0056 (14)	0.0082 (12)
C57B	0.036 (2)	0.036 (2)	0.035 (2)	−0.0097 (16)	−0.0085 (14)	0.0140 (13)
C58B	0.039 (2)	0.042 (2)	0.048 (3)	−0.0193 (17)	−0.0175 (16)	0.0251 (17)
Co2	0.02258 (16)	0.02273 (16)	0.01370 (15)	−0.00627 (12)	−0.00263 (11)	0.00283 (12)
Cl2	0.0329 (3)	0.0221 (3)	0.0218 (3)	−0.0075 (2)	−0.0041 (2)	−0.0025 (2)
Cl3	0.0258 (3)	0.0505 (4)	0.0179 (3)	−0.0077 (3)	−0.0066 (2)	0.0106 (3)
Cl4	0.0252 (3)	0.0254 (3)	0.0213 (3)	−0.0111 (2)	0.0018 (2)	0.0009 (2)

Geometric parameters (Å, º)

Co1—Cl1	2.2305 (6)	C34—H34	0.9500
Co1—P1	2.2495 (6)	C34—C35	1.387 (4)
Co1—P2	2.2515 (6)	C35—H35	0.9500
Co1—P3	2.2590 (6)	C35—C36	1.392 (3)
Co1—P4	2.2480 (6)	C36—H36	0.9500
P1—P2	2.6249 (7)	C37—C38	1.399 (3)
P1—N2	1.6842 (18)	C37—C42	1.402 (3)
P1—C25	1.816 (2)	C38—H38	0.9500
P1—C31	1.822 (2)	C38—C39	1.381 (3)
P2—N2	1.7004 (17)	C39—H39	0.9500
P2—C37	1.810 (2)	C39—C40	1.391 (3)
P2—C43	1.813 (2)	C40—H40	0.9500
P3—P4	2.6263 (7)	C40—C41	1.389 (4)
P3—N1	1.7071 (17)	C41—H41	0.9500
P3—C13	1.824 (2)	C41—C42	1.389 (3)
P3—C19	1.809 (2)	C42—H42	0.9500
P4—N1	1.6883 (18)	C43—C44	1.398 (3)
P4—C1	1.824 (2)	C43—C48	1.398 (3)
P4—C7	1.815 (2)	C44—H44	0.9500
N1—C49	1.490 (3)	C44—C45	1.392 (3)
N2—C54	1.479 (3)	C45—H45	0.9500
C1—C2	1.389 (3)	C45—C46	1.388 (4)
C1—C6	1.403 (3)	C46—H46	0.9500
C2—H2	0.9500	C46—C47	1.377 (4)
C2—C3	1.391 (3)	C47—H47	0.9500
C3—H3	0.9500	C47—C48	1.394 (3)
C3—C4	1.382 (4)	C48—H48	0.9500
C4—H4	0.9500	C49—H49a	0.9900
C4—C5	1.384 (4)	C49—H49b	0.9900
C5—H5	0.9500	C49—C50	1.524 (3)
C5—C6	1.392 (3)	C50—H50a	0.9900
C6—H6	0.9500	C50—H50b	0.9900
C7—C8	1.398 (3)	C50—C51	1.521 (3)
C7—C12	1.397 (3)	C51—H51a	0.9900
C8—H8	0.9500	C51—H51b	0.9900
C8—C9	1.390 (3)	C51—C52A	1.537 (12)
C9—H9	0.9500	C51—C52B	1.529 (10)

C9—C10	1.388 (3)	C52A—H52a	0.9900
C10—H10	0.9500	C52A—H52b	0.9900
C10—C11	1.391 (4)	C52A—C53A	1.528 (11)
C11—H11	0.9500	C53A—H53a	0.9800
C11—C12	1.391 (3)	C53A—H53b	0.9800
C12—H12	0.9500	C53A—H53c	0.9800
C13—C14	1.400 (3)	C52B—H52c	0.9900
C13—C18	1.397 (3)	C52B—H52d	0.9900
C14—H14	0.9500	C52B—C53B	1.515 (9)
C14—C15	1.390 (3)	C53B—H53d	0.9800
C15—H15	0.9500	C53B—H53e	0.9800
C15—C16	1.381 (3)	C53B—H53f	0.9800
C16—H16	0.9500	C54—H54a	0.9900
C16—C17	1.390 (3)	C54—H54b	0.9900
C17—H17	0.9500	C54—C55A	1.53 (2)
C17—C18	1.390 (3)	C54—C55B	1.512 (12)
C18—H18	0.9500	C55A—H55a	0.9900
C19—C20	1.397 (3)	C55A—H55b	0.9900
C19—C24	1.403 (3)	C55A—C56A	1.53 (2)
C20—H20	0.9500	C56A—H56a	0.9900
C20—C21	1.390 (3)	C56A—H56b	0.9900
C21—H21	0.9500	C56A—C57A	1.516 (11)
C21—C22	1.386 (4)	C57A—H57a	0.9900
C22—H22	0.9500	C57A—H57b	0.9900
C22—C23	1.388 (3)	C57A—C58A	1.505 (13)
C23—H23	0.9500	C58A—H58a	0.9800
C23—C24	1.390 (3)	C58A—H58b	0.9800
C24—H24	0.9500	C58A—H58c	0.9800
C25—C26	1.402 (3)	C55B—H55c	0.9900
C25—C30	1.393 (3)	C55B—H55d	0.9900
C26—H26	0.9500	C55B—C56B	1.556 (13)
C26—C27	1.388 (3)	C56B—H56c	0.9900
C27—H27	0.9500	C56B—H56d	0.9900
C27—C28	1.391 (4)	C56B—C57B	1.517 (8)
C28—H28	0.9500	C57B—H57c	0.9900
C28—C29	1.385 (3)	C57B—H57d	0.9900
C29—H29	0.9500	C57B—C58B	1.525 (6)
C29—C30	1.392 (3)	C58B—H58d	0.9800
C30—H30	0.9500	C58B—H58e	0.9800
C31—C32	1.396 (3)	C58B—H58f	0.9800
C31—C36	1.397 (3)	Co2—Cl2	2.2470 (6)
C32—H32	0.9500	Co2—Cl3	2.2292 (7)
C32—C33	1.388 (3)	Co2—Cl4	2.3411 (7)
C33—H33	0.9500	Co2—Cl4^{i}	2.3248 (6)
C33—C34	1.388 (3)		

P1—Co1—Cl1	95.27 (2)	H34—C34—C33	120.08 (14)
P2—Co1—Cl1	131.45 (3)	C35—C34—C33	119.8 (2)

P2—Co1—P1	71.35 (2)	C35—C34—H34	120.08 (14)
P3—Co1—Cl1	122.88 (2)	H35—C35—C34	119.86 (14)
P3—Co1—P1	103.72 (2)	C36—C35—C34	120.3 (2)
P3—Co1—P2	105.67 (2)	C36—C35—H35	119.86 (15)
P4—Co1—Cl1	94.10 (2)	C35—C36—C31	120.2 (2)
P4—Co1—P1	170.63 (2)	H36—C36—C31	119.91 (13)
P4—Co1—P2	101.97 (2)	H36—C36—C35	119.91 (15)
P4—Co1—P3	71.28 (2)	C38—C37—P2	120.48 (16)
P2—P1—Co1	54.361 (17)	C42—C37—P2	120.13 (17)
N2—P1—Co1	93.72 (6)	C42—C37—C38	119.4 (2)
N2—P1—P2	39.37 (6)	H38—C38—C37	119.77 (13)
C25—P1—Co1	120.42 (7)	C39—C38—C37	120.5 (2)
C25—P1—P2	124.48 (7)	C39—C38—H38	119.77 (14)
C25—P1—N2	108.47 (10)	H39—C39—C38	120.07 (14)
C31—P1—Co1	123.94 (7)	C40—C39—C38	119.9 (2)
C31—P1—P2	126.70 (7)	C40—C39—H39	120.07 (14)
C31—P1—N2	106.38 (9)	H40—C40—C39	119.86 (14)
C31—P1—C25	102.07 (10)	C41—C40—C39	120.3 (2)
P1—P2—Co1	54.290 (17)	C41—C40—H40	119.86 (14)
N2—P2—Co1	93.20 (6)	H41—C41—C40	119.95 (14)
N2—P2—P1	38.93 (6)	C42—C41—C40	120.1 (2)
C37—P2—Co1	125.72 (7)	C42—C41—H41	119.95 (14)
C37—P2—P1	125.62 (7)	C41—C42—C37	119.9 (2)
C37—P2—N2	106.28 (9)	H42—C42—C37	120.07 (13)
C43—P2—Co1	119.09 (8)	H42—C42—C41	120.07 (14)
C43—P2—P1	121.97 (7)	C44—C43—P2	117.86 (17)
C43—P2—N2	104.93 (9)	C48—C43—P2	122.22 (18)
C43—P2—C37	104.20 (10)	C48—C43—C44	119.6 (2)
P4—P3—Co1	54.163 (17)	H44—C44—C43	120.06 (13)
N1—P3—Co1	93.16 (6)	C45—C44—C43	119.9 (2)
N1—P3—P4	39.07 (6)	C45—C44—H44	120.06 (16)
C13—P3—Co1	119.46 (7)	H45—C45—C44	120.02 (16)
C13—P3—P4	124.39 (7)	C46—C45—C44	120.0 (2)
C13—P3—N1	106.10 (9)	C46—C45—H45	120.02 (15)
C19—P3—Co1	126.49 (7)	H46—C46—C45	119.72 (15)
C19—P3—P4	125.27 (7)	C47—C46—C45	120.6 (2)
C19—P3—N1	106.47 (9)	C47—C46—H46	119.72 (15)
C19—P3—C13	102.33 (10)	H47—C47—C46	119.96 (15)
P3—P4—Co1	54.553 (17)	C48—C47—C46	120.1 (2)
N1—P4—Co1	94.07 (6)	C48—C47—H47	119.96 (16)
N1—P4—P3	39.59 (6)	C47—C48—C43	119.9 (2)
C1—P4—Co1	119.68 (7)	H48—C48—C43	120.04 (14)
C1—P4—P3	126.39 (7)	H48—C48—C47	120.04 (16)
C1—P4—N1	107.66 (9)	H49a—C49—N1	108.26 (11)
C7—P4—Co1	119.31 (7)	H49b—C49—N1	108.26 (11)
C7—P4—P3	125.49 (7)	H49b—C49—H49a	107.4
C7—P4—N1	111.37 (10)	C50—C49—N1	116.09 (18)
C7—P4—C1	103.97 (10)	C50—C49—H49a	108.26 (12)

P4—N1—P3	101.33 (9)	C50—C49—H49b	108.26 (12)
C49—N1—P3	126.83 (14)	H50a—C50—C49	108.67 (12)
C49—N1—P4	131.83 (14)	H50b—C50—C49	108.67 (12)
P2—N2—P1	101.70 (9)	H50b—C50—H50a	107.6
C54—N2—P1	128.88 (14)	C51—C50—C49	114.36 (19)
C54—N2—P2	128.92 (14)	C51—C50—H50a	108.67 (13)
C2—C1—P4	122.83 (17)	C51—C50—H50b	108.67 (12)
C6—C1—P4	118.18 (16)	H51a—C51—C50	110.26 (13)
C6—C1—C2	119.0 (2)	H51b—C51—C50	110.26 (12)
H2—C2—C1	119.79 (14)	H51b—C51—H51a	108.5
C3—C2—C1	120.4 (2)	C52A—C51—C50	120.2 (7)
C3—C2—H2	119.79 (15)	C52A—C51—H51a	103.4 (7)
H3—C3—C2	119.86 (15)	C52A—C51—H51b	103.5 (7)
C4—C3—C2	120.3 (2)	C52B—C51—C50	107.3 (6)
C4—C3—H3	119.86 (14)	C52B—C51—H51a	110.3 (6)
H4—C4—C3	119.97 (14)	C52B—C51—H51b	110.3 (6)
C5—C4—C3	120.1 (2)	C52B—C51—C52A	12.9 (6)
C5—C4—H4	119.97 (15)	H52a—C52A—C51	108.8 (7)
H5—C5—C4	119.99 (15)	H52b—C52A—C51	108.8 (7)
C6—C5—C4	120.0 (2)	H52b—C52A—H52a	107.7
C6—C5—H5	119.99 (14)	C53A—C52A—C51	113.8 (9)
C5—C6—C1	120.2 (2)	C53A—C52A—H52a	108.8 (8)
H6—C6—C1	119.88 (13)	C53A—C52A—H52b	108.8 (6)
H6—C6—C5	119.88 (14)	H53a—C53A—C52A	109.5
C8—C7—P4	116.47 (16)	H53b—C53A—C52A	109.5
C12—C7—P4	124.40 (17)	H53b—C53A—H53a	109.5
C12—C7—C8	119.1 (2)	H53c—C53A—C52A	109.5
H8—C8—C7	119.55 (13)	H53c—C53A—H53a	109.5
C9—C8—C7	120.9 (2)	H53c—C53A—H53b	109.5
C9—C8—H8	119.55 (14)	H52c—C52B—C51	109.7 (6)
H9—C9—C8	120.12 (14)	H52d—C52B—C51	109.7 (6)
C10—C9—C8	119.8 (2)	H52d—C52B—H52c	108.2
C10—C9—H9	120.12 (13)	C53B—C52B—C51	109.7 (7)
H10—C10—C9	120.16 (13)	C53B—C52B—H52c	109.7 (6)
C11—C10—C9	119.7 (2)	C53B—C52B—H52d	109.7 (5)
C11—C10—H10	120.16 (14)	H53d—C53B—C52B	109.5
H11—C11—C10	119.58 (14)	H53e—C53B—C52B	109.5
C12—C11—C10	120.8 (2)	H53e—C53B—H53d	109.5
C12—C11—H11	119.58 (14)	H53f—C53B—C52B	109.5
C11—C12—C7	119.7 (2)	H53f—C53B—H53d	109.5
H12—C12—C7	120.14 (13)	H53f—C53B—H53e	109.5
H12—C12—C11	120.14 (14)	H54a—C54—N2	108.09 (11)
C14—C13—P3	118.05 (16)	H54b—C54—N2	108.09 (11)
C18—C13—P3	122.44 (16)	H54b—C54—H54a	107.3
C18—C13—C14	119.44 (19)	C55A—C54—N2	115.3 (8)
H14—C14—C13	120.12 (12)	C55A—C54—H54a	113.8 (9)
C15—C14—C13	119.8 (2)	C55A—C54—H54b	103.9 (10)
C15—C14—H14	120.12 (14)	C55B—C54—N2	116.8 (5)

H15—C15—C14	119.74 (14)	C55B—C54—H54a	108.1 (5)
C16—C15—C14	120.5 (2)	C55B—C54—H54b	108.1 (6)
C16—C15—H15	119.74 (13)	C55B—C54—C55A	6.0 (14)
H16—C16—C15	119.93 (13)	H55a—C55A—C54	109.5 (9)
C17—C16—C15	120.1 (2)	H55b—C55A—C54	109.5 (10)
C17—C16—H16	119.93 (13)	H55b—C55A—H55a	108.0518 (1)
H17—C17—C16	120.02 (13)	C56A—C55A—C54	110.9 (15)
C18—C17—C16	120.0 (2)	C56A—C55A—H55a	109.5 (10)
C18—C17—H17	120.02 (14)	C56A—C55A—H55b	109.5 (10)
C17—C18—C13	120.2 (2)	H56a—C56A—C55A	108.3 (9)
H18—C18—C13	119.91 (12)	H56b—C56A—C55A	108.3 (10)
H18—C18—C17	119.91 (14)	H56b—C56A—H56a	107.4
C20—C19—P3	121.61 (16)	C57A—C56A—C55A	115.9 (12)
C24—C19—P3	119.21 (16)	C57A—C56A—H56a	108.3 (4)
C24—C19—C20	119.2 (2)	C57A—C56A—H56b	108.3 (5)
H20—C20—C19	119.98 (13)	H57a—C57A—C56A	108.9 (4)
C21—C20—C19	120.0 (2)	H57b—C57A—C56A	108.9 (4)
C21—C20—H20	119.98 (14)	H57b—C57A—H57a	107.7
H21—C21—C20	119.76 (14)	C58A—C57A—C56A	113.4 (8)
C22—C21—C20	120.5 (2)	C58A—C57A—H57a	108.9 (5)
C22—C21—H21	119.76 (14)	C58A—C57A—H57b	108.9 (5)
H22—C22—C21	120.02 (14)	H58a—C58A—C57A	109.5
C23—C22—C21	120.0 (2)	H58b—C58A—C57A	109.5
C23—C22—H22	120.02 (14)	H58b—C58A—H58a	109.5
H23—C23—C22	119.96 (14)	H58c—C58A—C57A	109.5
C24—C23—C22	120.1 (2)	H58c—C58A—H58a	109.5
C24—C23—H23	119.96 (14)	H58c—C58A—H58b	109.5
C23—C24—C19	120.3 (2)	H55c—C55B—C54	109.9 (5)
H24—C24—C19	119.87 (13)	H55d—C55B—C54	109.9 (6)
H24—C24—C23	119.87 (14)	H55d—C55B—H55c	108.3
C26—C25—P1	118.95 (16)	C56B—C55B—C54	108.8 (9)
C30—C25—P1	122.02 (16)	C56B—C55B—H55c	109.9 (5)
C30—C25—C26	119.0 (2)	C56B—C55B—H55d	109.9 (6)
H26—C26—C25	120.01 (13)	H56c—C56B—C55B	108.4 (5)
C27—C26—C25	120.0 (2)	H56d—C56B—C55B	108.4 (5)
C27—C26—H26	120.01 (14)	H56d—C56B—H56c	107.5
H27—C27—C26	119.63 (14)	C57B—C56B—C55B	115.5 (7)
C28—C27—C26	120.7 (2)	C57B—C56B—H56c	108.4 (3)
C28—C27—H27	119.63 (14)	C57B—C56B—H56d	108.4 (3)
H28—C28—C27	120.32 (14)	H57c—C57B—C56B	109.4 (3)
C29—C28—C27	119.4 (2)	H57d—C57B—C56B	109.4 (3)
C29—C28—H28	120.32 (14)	H57d—C57B—H57c	108.0
H29—C29—C28	119.79 (14)	C58B—C57B—C56B	111.0 (4)
C30—C29—C28	120.4 (2)	C58B—C57B—H57c	109.4 (3)
C30—C29—H29	119.79 (14)	C58B—C57B—H57d	109.4 (3)
C29—C30—C25	120.4 (2)	H58d—C58B—C57B	109.5
H30—C30—C25	119.78 (13)	H58e—C58B—C57B	109.5
H30—C30—C29	119.78 (14)	H58e—C58B—H58d	109.5

C32—C31—P1	120.12 (16)	H58f—C58B—C57B	109.5
C36—C31—P1	120.82 (17)	H58f—C58B—H58d	109.5
C36—C31—C32	119.0 (2)	H58f—C58B—H58e	109.5
H32—C32—C31	119.72 (13)	Cl3—Co2—Cl2	114.97 (3)
C33—C32—C31	120.6 (2)	Cl4—Co2—Cl2	114.46 (2)
C33—C32—H32	119.72 (14)	Cl4^{i}—Co2—Cl2	110.84 (2)
H33—C33—C32	119.95 (14)	Cl4^{i}—Co2—Cl3	111.82 (2)
C34—C33—C32	120.1 (2)	Cl4—Co2—Cl3	108.67 (3)
C34—C33—H33	119.95 (14)		

Co1—P1—N2—P2	−1.57 (5)	N2—P2—C43—C44	−83.68 (14)
Co1—P1—N2—C54	170.79 (12)	N2—P2—C43—C48	89.71 (14)
Co1—P1—C25—C26	−68.58 (12)	N2—C54—C55A—C56A	165.7 (12)
Co1—P1—C25—C30	111.81 (13)	N2—C54—C55B—C56B	−166.6 (7)
Co1—P1—C31—C32	−24.75 (12)	C1—P4—N1—C49	53.97 (14)
Co1—P1—C31—C36	158.52 (16)	C1—P4—C7—C8	76.36 (14)
Co1—P2—N2—P1	1.56 (5)	C1—P4—C7—C12	−106.08 (15)
Co1—P2—N2—C54	−170.78 (12)	C1—C2—C3—C4	−0.3 (3)
Co1—P2—C37—C38	−87.57 (13)	C1—C6—C5—C4	−1.2 (3)
Co1—P2—C37—C42	92.27 (14)	C2—C1—P4—C7	−2.2 (2)
Co1—P2—C43—C44	18.70 (11)	C2—C1—C6—C5	0.6 (3)
Co1—P2—C43—C48	−167.91 (14)	C2—C3—C4—C5	−0.2 (3)
Co1—P3—N1—P4	3.35 (5)	C3—C2—C1—C6	0.1 (3)
Co1—P3—N1—C49	−176.91 (12)	C3—C4—C5—C6	0.9 (3)
Co1—P3—C13—C14	7.49 (11)	C6—C1—P4—C7	178.29 (17)
Co1—P3—C13—C18	−175.74 (14)	C7—P4—N1—C49	−59.39 (14)
Co1—P3—C19—C20	−88.84 (13)	C7—C8—C9—C10	0.5 (3)
Co1—P3—C19—C24	89.40 (13)	C7—C12—C11—C10	0.1 (3)
Co1—P4—N1—P3	−3.37 (5)	C8—C7—C12—C11	0.3 (2)
Co1—P4—N1—C49	176.91 (12)	C8—C9—C10—C11	−0.1 (3)
Co1—P4—C1—C2	134.09 (15)	C9—C8—C7—C12	−0.6 (3)
Co1—P4—C1—C6	−45.46 (12)	C9—C10—C11—C12	−0.2 (3)
Co1—P4—C7—C8	−60.10 (12)	C13—P3—N1—C49	−55.00 (14)
Co1—P4—C7—C12	117.46 (15)	C13—P3—C19—C20	129.16 (14)
P1—P2—N2—C54	−172.35 (12)	C13—P3—C19—C24	−52.60 (13)
P1—P2—C37—C38	−19.23 (11)	C13—C14—C15—C16	−0.7 (3)
P1—P2—C37—C42	160.61 (15)	C13—C18—C17—C16	−0.6 (2)
P1—P2—C43—C44	−45.19 (12)	C14—C13—P3—C19	152.85 (17)
P1—P2—C43—C48	128.20 (14)	C14—C13—C18—C17	0.3 (2)
P1—N2—P2—C37	−127.16 (10)	C14—C15—C16—C17	0.4 (3)
P1—N2—P2—C43	122.82 (10)	C15—C14—C13—C18	0.4 (3)
P1—N2—C54—C55A	−96.8 (11)	C15—C16—C17—C18	0.3 (3)
P1—N2—C54—C55B	−90.3 (6)	C18—C13—P3—C19	−30.39 (19)
P1—C25—C26—C27	−179.13 (17)	C19—P3—N1—C49	53.49 (14)
P1—C25—C30—C29	177.44 (17)	C19—C20—C21—C22	−1.4 (3)
P1—C31—C32—C33	−178.75 (17)	C19—C24—C23—C22	−0.4 (3)
P1—C31—C36—C35	177.3 (2)	C20—C19—C24—C23	−0.2 (2)
P2—P1—N2—C54	172.35 (12)	C20—C21—C22—C23	0.8 (3)

P2—P1—C25—C26	−133.97 (14)	C21—C20—C19—C24	1.1 (3)
P2—P1—C25—C30	46.42 (12)	C21—C22—C23—C24	0.1 (3)
P2—P1—C31—C32	43.27 (12)	C25—P1—N2—C54	−65.39 (14)
P2—P1—C31—C36	−133.47 (16)	C25—P1—C31—C32	−164.92 (15)
P2—N2—P1—C25	122.26 (10)	C25—P1—C31—C36	18.34 (15)
P2—N2—P1—C31	−128.60 (10)	C25—C26—C27—C28	1.3 (3)
P2—N2—C54—C55A	73.6 (11)	C25—C30—C29—C28	2.1 (3)
P2—N2—C54—C55B	80.0 (6)	C26—C25—P1—C31	73.39 (18)
P2—C37—C38—C39	−178.56 (17)	C26—C25—C30—C29	−2.2 (2)
P2—C37—C42—C41	179.90 (18)	C26—C27—C28—C29	−1.4 (3)
P2—C43—C44—C45	173.70 (17)	C27—C26—C25—C30	0.5 (3)
P2—C43—C48—C47	−172.81 (18)	C27—C28—C29—C30	−0.3 (3)
P3—P4—N1—C49	−179.72 (12)	C30—C25—P1—C31	−106.23 (18)
P3—P4—C1—C2	−160.06 (16)	C31—P1—N2—C54	43.75 (14)
P3—P4—C1—C6	20.39 (11)	C31—C32—C33—C34	1.4 (3)
P3—P4—C7—C8	−125.48 (14)	C31—C36—C35—C34	1.6 (3)
P3—P4—C7—C12	52.08 (13)	C32—C31—C36—C35	0.5 (3)
P3—N1—P4—C1	−126.30 (10)	C32—C33—C34—C35	0.7 (3)
P3—N1—P4—C7	120.33 (10)	C33—C32—C31—C36	−2.0 (3)
P3—N1—C49—C50	117.94 (18)	C33—C34—C35—C36	−2.1 (3)
P3—C13—C14—C15	177.24 (16)	C37—P2—N2—C54	60.49 (14)
P3—C13—C18—C17	−176.45 (17)	C37—P2—C43—C44	164.80 (15)
P3—C19—C20—C21	179.33 (18)	C37—P2—C43—C48	−21.81 (14)
P3—C19—C24—C23	−178.50 (17)	C37—C38—C39—C40	−1.7 (3)
P4—P3—N1—C49	179.74 (11)	C37—C42—C41—C40	−0.9 (3)
P4—P3—C13—C14	−57.15 (12)	C38—C37—P2—C43	129.32 (18)
P4—P3—C13—C18	119.61 (14)	C38—C37—C42—C41	−0.3 (2)
P4—P3—C19—C20	−20.48 (11)	C38—C39—C40—C41	0.5 (3)
P4—P3—C19—C24	157.75 (15)	C39—C38—C37—C42	1.6 (3)
P4—N1—P3—C13	125.26 (10)	C39—C40—C41—C42	0.8 (3)
P4—N1—P3—C19	−126.25 (10)	C42—C37—P2—C43	−50.83 (19)
P4—N1—C49—C50	−62.4 (2)	C43—P2—N2—C54	−49.53 (14)
P4—C1—C2—C3	−179.4 (2)	C43—C44—C45—C46	−0.7 (3)
P4—C1—C6—C5	−179.79 (18)	C43—C48—C47—C46	−0.5 (3)
P4—C7—C8—C9	177.12 (16)	C44—C43—C48—C47	0.5 (2)
P4—C7—C12—C11	−177.2 (2)	C44—C45—C46—C47	0.6 (3)
N1—P3—C13—C14	−95.74 (14)	C45—C44—C43—C48	0.1 (3)
N1—P3—C13—C18	81.03 (13)	C45—C46—C47—C48	0.0 (3)
N1—P3—C19—C20	18.03 (13)	C49—C50—C51—C52A	−177.3 (8)
N1—P3—C19—C24	−163.74 (14)	C49—C50—C51—C52B	−177.4 (6)
N1—P4—C1—C2	−120.42 (16)	C50—C51—C52A—C53A	175.6 (8)
N1—P4—C1—C6	60.04 (14)	C50—C51—C52B—C53B	−179.0 (6)
N1—P4—C7—C8	−167.98 (15)	C52A—C51—C52B—C53B	1 (6)
N1—P4—C7—C12	9.58 (14)	C53A—C52A—C51—C52B	176 (2)
N1—C49—C50—C51	−71.4 (2)	C54—C55A—C56A—C57A	56.1 (17)
N2—P1—C25—C26	−174.57 (14)	C54—C55B—C56B—C57B	72.0 (9)
N2—P1—C25—C30	5.82 (13)	C55A—C54—C55B—C56B	−91 (13)
N2—P1—C31—C32	81.46 (14)	C55A—C56A—C57A—C58A	56.5 (13)

N2—P1—C31—C36	−95.27 (15)	C56A—C55A—C54—C55B	59 (4)
N2—P2—C37—C38	18.79 (13)	C55B—C56B—C57B—C58B	−168.2 (7)
N2—P2—C37—C42	−161.37 (15)		

Symmetry code: (i) −*x*, −*y*, −*z*+1.

Bis[bis(diphenylphosphanyl)(propan-2-yl)amine-κ^2P,P']\ chloridocobalt(III) di-μ-chlorido-bis[dichloridocobalt(II)] (2)

Crystal data

$[CoCl(C_{27}H_{27}NP_2)_2][Co_2Cl_6]$
M_r = 1279.90
Monoclinic, $P2_1/c$
a = 12.2179 (2) Å
b = 15.4508 (2) Å
c = 30.4455 (5) Å
β = 97.070 (1)°
V = 5703.69 (15) Å^3
Z = 4
$F(000)$ = 2303.850
D_x = 1.490 Mg m^{-3}
Mo $K\alpha$ radiation, λ = 0.71073 Å
Cell parameters from 8203 reflections
θ = 2.1–28.5°
μ = 1.34 mm^{-1}
T = 100 K
Block, green
0.40 × 0.18 × 0.14 mm

Data collection

Bruker SMART APEXII area detector diffractometer
Radiation source: microfocus sealed X-ray tube, Incoatec Iμs
Mirror optics monochromator
Detector resolution: 7.9 pixels mm^{-1}
ω and φ scans
Absorption correction: multi-scan (SADABS; Bruker, 2009)
T_{min} = 0.672, T_{max} = 0.746
131209 measured reflections
14218 independent reflections
11950 reflections with $I \geq 2u(I)$
R_{int} = 0.029
θ_{max} = 28.4°, θ_{min} = 1.7°
h = −15→16
k = −20→20
l = −40→40

Refinement

Refinement on F^2
Least-squares matrix: full
$R[F^2 > 2\sigma(F^2)]$ = 0.030
$wR(F^2)$ = 0.077
S = 1.05
14218 reflections
629 parameters
96 restraints
111 constraints
Primary atom site location: structure-invariant direct methods
H-atom parameters constrained
$w = 1/[\sigma^2(F_o^2) + (0.031P)^2 + 4.9409P]$ where $P = (F_o^2 + 2F_c^2)/3$
$(\Delta/\sigma)_{max}$ = −0.0001
$\Delta\rho_{max}$ = 0.50 e Å^{-3}
$\Delta\rho_{min}$ = −0.35 e Å^{-3}

Fractional atomic coordinates and isotropic or equivalent isotropic displacement parameters (Å^2)

	x	y	z	U_{iso}*/U_{eq}	Occ. (<1)
Co1	0.118373 (16)	0.333819 (13)	0.180200 (7)	0.01410 (5)	
Cl1	0.08020 (3)	0.45086 (3)	0.218974 (13)	0.02277 (8)	
P1	0.08860 (3)	0.29287 (3)	0.109708 (13)	0.01694 (8)	
P2	0.22859 (3)	0.40951 (3)	0.141564 (14)	0.01670 (8)	
P3	0.01308 (3)	0.23811 (3)	0.212661 (13)	0.01431 (8)	
P4	0.23163 (3)	0.23556 (3)	0.219602 (13)	0.01372 (8)	
N1	0.18661 (11)	0.35955 (9)	0.09282 (4)	0.0184 (3)	
N2	0.12288 (10)	0.18490 (8)	0.23936 (4)	0.0145 (2)	

C1	−0.04727 (14)	0.32779 (11)	0.08433 (5)	0.0208 (3)	
C2	−0.09873 (15)	0.29587 (13)	0.04385 (6)	0.0274 (4)	
H2	−0.06111 (15)	0.25590 (13)	0.02733 (6)	0.0329 (5)*	
C3	−0.20496 (17)	0.32279 (15)	0.02786 (7)	0.0354 (5)	
H3	−0.24035 (17)	0.29990 (15)	0.00081 (7)	0.0425 (5)*	
C4	−0.25921 (17)	0.38258 (15)	0.05110 (7)	0.0380 (5)	
H4	−0.33175 (17)	0.40052 (15)	0.04001 (7)	0.0456 (6)*	
C5	−0.20790 (16)	0.41665 (14)	0.09073 (7)	0.0327 (4)	
H5	−0.24430 (16)	0.45901 (14)	0.10629 (7)	0.0393 (5)*	
C6	−0.10309 (14)	0.38821 (12)	0.10734 (6)	0.0251 (4)	
H6	−0.06891 (14)	0.41025 (12)	0.13478 (6)	0.0301 (4)*	
C7A	0.1952 (5)	0.3821 (4)	0.04546 (19)	0.0266 (11)	0.793 (5)
H7A	0.1687 (5)	0.3303 (4)	0.02758 (19)	0.0319 (13)*	0.793 (5)
C8A	0.1208 (6)	0.4574 (5)	0.0280 (2)	0.0309 (11)	0.793 (5)
H8Aa	0.1156 (16)	0.4592 (10)	−0.0044 (2)	0.0464 (17)*	0.793 (5)
H8Ab	0.0471 (8)	0.4493 (9)	0.0369 (7)	0.0464 (17)*	0.793 (5)
H8Ac	0.1521 (11)	0.5119 (5)	0.0403 (6)	0.0464 (17)*	0.793 (5)
C9A	0.3130 (2)	0.39805 (17)	0.03629 (8)	0.0313 (6)	0.793 (5)
H9Aa	0.3559 (4)	0.3447 (4)	0.0416 (6)	0.0469 (10)*	0.793 (5)
H9Ab	0.3130 (2)	0.4159 (12)	0.00541 (19)	0.0469 (10)*	0.793 (5)
H9Ac	0.3461 (6)	0.4438 (9)	0.0559 (4)	0.0469 (10)*	0.793 (5)
C7B	0.201 (2)	0.3969 (15)	0.0474 (7)	0.022 (3)	0.207 (5)
H7B	0.270 (2)	0.4314 (15)	0.0516 (7)	0.026 (4)*	0.207 (5)
C8B	0.109 (2)	0.4610 (19)	0.0329 (9)	0.024 (3)	0.207 (5)
H8Ba	0.130 (3)	0.497 (4)	0.0089 (19)	0.036 (5)*	0.207 (5)
H8Bb	0.041 (3)	0.4295 (19)	0.023 (2)	0.036 (5)*	0.207 (5)
H8Bc	0.096 (5)	0.498 (4)	0.0580 (11)	0.036 (5)*	0.207 (5)
C9B	0.2184 (7)	0.3275 (5)	0.0147 (2)	0.0213 (19)	0.207 (5)
H9Ba	0.159 (3)	0.285 (2)	0.0139 (15)	0.032 (3)*	0.207 (5)
H9Bb	0.218 (5)	0.3532 (8)	−0.0148 (5)	0.032 (3)*	0.207 (5)
H9Bc	0.289 (2)	0.299 (3)	0.0235 (12)	0.032 (3)*	0.207 (5)
C10	0.11081 (14)	0.18935 (11)	0.08442 (5)	0.0212 (3)	
C11	0.21318 (15)	0.17051 (12)	0.07068 (7)	0.0288 (4)	
H11	0.27184 (15)	0.21107 (12)	0.07568 (7)	0.0346 (5)*	
C12	0.22917 (18)	0.09255 (14)	0.04971 (8)	0.0399 (5)	
H12	0.29828 (18)	0.08062 (14)	0.03973 (8)	0.0479 (6)*	
C13	0.14502 (18)	0.03199 (14)	0.04324 (8)	0.0388 (5)	
H13	0.15620 (18)	−0.02095 (14)	0.02856 (8)	0.0466 (6)*	
C14	0.04473 (17)	0.04881 (13)	0.05819 (7)	0.0330 (4)	
H14	−0.01220 (17)	0.00659 (13)	0.05458 (7)	0.0397 (5)*	
C15	0.02702 (15)	0.12720 (12)	0.07846 (6)	0.0255 (4)	
H15	−0.04234 (15)	0.13870 (12)	0.08833 (6)	0.0306 (4)*	
C16	0.21212 (15)	0.52458 (11)	0.13023 (6)	0.0218 (3)	
C17	0.10814 (16)	0.56253 (12)	0.12732 (7)	0.0300 (4)	
H17	0.04866 (16)	0.53168 (12)	0.13732 (7)	0.0360 (5)*	
C18	0.09069 (18)	0.64520 (13)	0.10987 (7)	0.0352 (5)	
H18	0.01937 (18)	0.67048 (13)	0.10788 (7)	0.0422 (5)*	
C19	0.17700 (17)	0.69084 (12)	0.09538 (6)	0.0296 (4)	

H19	0.16458 (17)	0.74680 (12)	0.08281 (6)	0.0355 (5)*
C20	0.28139 (16)	0.65470 (12)	0.09925 (6)	0.0272 (4)
H20	0.34086 (16)	0.68642 (12)	0.08980 (6)	0.0326 (4)*
C21	0.29965 (15)	0.57239 (11)	0.11686 (6)	0.0237 (3)
H21	0.37177 (15)	0.54837 (11)	0.11986 (6)	0.0284 (4)*
C22	0.37588 (13)	0.39809 (11)	0.15757 (6)	0.0209 (3)
C23	0.41854 (15)	0.43729 (13)	0.19729 (6)	0.0294 (4)
H23	0.37144 (15)	0.46996 (13)	0.21359 (6)	0.0353 (5)*
C24	0.52955 (18)	0.42877 (15)	0.21309 (8)	0.0410 (5)
H24	0.55812 (18)	0.45470 (15)	0.24041 (8)	0.0492 (6)*
C25	0.59834 (17)	0.38249 (14)	0.18899 (9)	0.0457 (6)
H25	0.67457 (17)	0.37755 (14)	0.19952 (9)	0.0548 (7)*
C26	0.55725 (17)	0.34372 (14)	0.15001 (10)	0.0443 (6)
H26	0.60516 (17)	0.31209 (14)	0.13362 (10)	0.0532 (7)*
C27	0.44518 (15)	0.35035 (12)	0.13413 (7)	0.0315 (4)
H27	0.41671 (15)	0.32224 (12)	0.10740 (7)	0.0378 (5)*
C28	−0.07196 (12)	0.16052 (11)	0.17905 (5)	0.0180 (3)
C29	−0.05171 (14)	0.07190 (11)	0.18095 (5)	0.0212 (3)
H29	0.00959 (14)	0.04984 (11)	0.19986 (5)	0.0254 (4)*
C30	−0.12158 (16)	0.01556 (13)	0.15504 (6)	0.0285 (4)
H30	−0.10802 (16)	−0.04498 (13)	0.15649 (6)	0.0342 (5)*
C31	−0.21063 (16)	0.04740 (14)	0.12721 (6)	0.0314 (4)
H31	−0.25727 (16)	0.00865 (14)	0.10936 (6)	0.0376 (5)*
C32	−0.23212 (14)	0.13542 (14)	0.12525 (6)	0.0292 (4)
H32	−0.29343 (14)	0.15706 (14)	0.10620 (6)	0.0350 (5)*
C33	−0.16337 (13)	0.19194 (12)	0.15134 (5)	0.0225 (3)
H33	−0.17852 (13)	0.25226 (12)	0.15037 (5)	0.0270 (4)*
C34	−0.07857 (13)	0.26699 (11)	0.25355 (5)	0.0192 (3)
C35	−0.17968 (16)	0.22495 (15)	0.25458 (7)	0.0352 (5)
H35	−0.20079 (16)	0.17955 (15)	0.23424 (7)	0.0422 (6)*
C36	−0.24956 (17)	0.24936 (19)	0.28531 (8)	0.0465 (6)
H36	−0.31811 (17)	0.22053 (19)	0.28571 (8)	0.0558 (7)*
C37	−0.22027 (17)	0.31455 (14)	0.31492 (7)	0.0363 (5)
H37	−0.26913 (17)	0.33185 (14)	0.33527 (7)	0.0435 (6)*
C38	−0.11941 (18)	0.35508 (12)	0.31510 (7)	0.0343 (5)
H38	−0.09803 (18)	0.39914 (12)	0.33618 (7)	0.0411 (5)*
C39	−0.04891 (17)	0.33154 (12)	0.28446 (6)	0.0281 (4)
H39	0.02012 (17)	0.35995 (12)	0.28472 (6)	0.0338 (5)*
C40	0.11738 (13)	0.12285 (10)	0.27705 (5)	0.0180 (3)
H40	0.03967 (13)	0.10144 (10)	0.27496 (5)	0.0216 (4)*
C41	0.19095 (14)	0.04388 (11)	0.27395 (6)	0.0239 (3)
H41a	0.1707 (7)	0.0149 (5)	0.24548 (19)	0.0359 (5)*
H41b	0.26822 (17)	0.06226 (15)	0.2763 (4)	0.0359 (5)*
H41c	0.1812 (8)	0.0037 (4)	0.2981 (3)	0.0359 (5)*
C42	0.14337 (14)	0.16632 (12)	0.32216 (5)	0.0242 (3)
H42a	0.2208 (3)	0.1846 (8)	0.32630 (19)	0.0364 (5)*
H42b	0.0957 (8)	0.2170 (5)	0.32362 (17)	0.0364 (5)*
H42c	0.1304 (11)	0.1253 (3)	0.34550 (6)	0.0364 (5)*

C43	0.32669 (12)	0.26922 (10)	0.26748 (5)	0.0169 (3)
C44	0.31033 (14)	0.35011 (11)	0.28572 (6)	0.0222 (3)
H44	0.25293 (14)	0.38659 (11)	0.27248 (6)	0.0266 (4)*
C45	0.37762 (15)	0.37770 (13)	0.32322 (6)	0.0299 (4)
H45	0.36590 (15)	0.43292 (13)	0.33554 (6)	0.0359 (5)*
C46	0.46166 (15)	0.32515 (14)	0.34270 (6)	0.0312 (4)
H46	0.50802 (15)	0.34452 (14)	0.36815 (6)	0.0374 (5)*
C47	0.47801 (14)	0.24428 (13)	0.32503 (6)	0.0267 (4)
H47	0.53505 (14)	0.20788 (13)	0.33863 (6)	0.0320 (4)*
C48	0.41129 (13)	0.21613 (11)	0.28746 (6)	0.0211 (3)
H48	0.42318 (13)	0.16076 (11)	0.27533 (6)	0.0253 (4)*
C49	0.30955 (13)	0.15562 (10)	0.19244 (5)	0.0176 (3)
C50	0.25762 (15)	0.08379 (11)	0.17158 (6)	0.0246 (4)
H50	0.18228 (15)	0.07256 (11)	0.17426 (6)	0.0295 (4)*
C51	0.31575 (18)	0.02834 (12)	0.14677 (7)	0.0327 (4)
H51	0.28039 (18)	−0.02136 (12)	0.13323 (7)	0.0393 (5)*
C52	0.42461 (18)	0.04526 (13)	0.14175 (7)	0.0347 (5)
H52	0.46360 (18)	0.00784 (13)	0.12440 (7)	0.0416 (6)*
C53	0.47660 (16)	0.11689 (14)	0.16210 (7)	0.0325 (4)
H53	0.55142 (16)	0.12861 (14)	0.15869 (7)	0.0390 (5)*
C54	0.41963 (14)	0.17179 (12)	0.18752 (6)	0.0249 (4)
H54	0.45596 (14)	0.22058 (12)	0.20161 (6)	0.0298 (4)*
Co2	0.550075 (19)	0.098443 (15)	−0.001164 (7)	0.02030 (5)
Cl2	0.65770 (4)	0.14151 (3)	−0.051121 (15)	0.02886 (9)
Cl3	0.50923 (4)	0.20213 (3)	0.044980 (15)	0.02943 (10)
Cl4	0.60392 (4)	−0.02764 (3)	0.038297 (14)	0.02537 (9)

Atomic displacement parameters (Å²)

	U^{11}	U^{22}	U^{33}	U^{12}	U^{13}	U^{23}
Co1	0.01223 (10)	0.01511 (10)	0.01540 (10)	0.00101 (7)	0.00353 (7)	0.00093 (8)
Cl1	0.0283 (2)	0.01768 (18)	0.02391 (19)	0.00526 (15)	0.00974 (16)	−0.00014 (14)
P1	0.01553 (19)	0.0199 (2)	0.01562 (18)	0.00082 (15)	0.00296 (14)	0.00085 (15)
P2	0.01565 (19)	0.01631 (19)	0.01900 (19)	0.00056 (14)	0.00561 (14)	0.00214 (15)
P3	0.01087 (17)	0.01686 (19)	0.01545 (18)	0.00012 (14)	0.00262 (13)	0.00081 (14)
P4	0.01090 (17)	0.01503 (18)	0.01548 (18)	−0.00001 (14)	0.00260 (13)	0.00082 (14)
N1	0.0196 (7)	0.0198 (7)	0.0167 (6)	−0.0002 (5)	0.0052 (5)	0.0019 (5)
N2	0.0114 (6)	0.0165 (6)	0.0159 (6)	−0.0006 (5)	0.0021 (5)	0.0018 (5)
C1	0.0184 (8)	0.0262 (8)	0.0177 (7)	0.0011 (6)	0.0024 (6)	0.0047 (6)
C2	0.0265 (9)	0.0362 (10)	0.0191 (8)	0.0011 (8)	0.0008 (7)	0.0028 (7)
C3	0.0298 (10)	0.0490 (12)	0.0250 (9)	−0.0001 (9)	−0.0061 (8)	0.0046 (9)
C4	0.0243 (10)	0.0526 (13)	0.0353 (11)	0.0078 (9)	−0.0035 (8)	0.0104 (10)
C5	0.0248 (9)	0.0409 (11)	0.0326 (10)	0.0103 (8)	0.0043 (8)	0.0053 (8)
C6	0.0209 (8)	0.0313 (9)	0.0231 (8)	0.0032 (7)	0.0028 (6)	0.0029 (7)
C7A	0.0309 (17)	0.031 (2)	0.0193 (16)	0.0061 (13)	0.0092 (10)	0.0079 (14)
C8A	0.035 (2)	0.0353 (19)	0.025 (2)	0.0098 (12)	0.0111 (14)	0.0119 (15)
C9A	0.0359 (13)	0.0327 (13)	0.0281 (12)	0.0069 (9)	0.0155 (9)	0.0075 (9)
C7B	0.025 (5)	0.026 (5)	0.016 (4)	−0.004 (3)	0.004 (2)	0.002 (2)

C8B	0.029 (6)	0.031 (5)	0.014 (5)	0.001 (3)	0.007 (3)	0.007 (3)
C9B	0.023 (4)	0.026 (4)	0.015 (3)	−0.004 (2)	0.005 (2)	0.002 (2)
C10	0.0231 (8)	0.0222 (8)	0.0179 (7)	0.0016 (6)	0.0015 (6)	−0.0011 (6)
C11	0.0227 (9)	0.0283 (9)	0.0357 (10)	0.0007 (7)	0.0046 (7)	−0.0049 (8)
C12	0.0281 (10)	0.0382 (12)	0.0545 (13)	0.0062 (9)	0.0096 (9)	−0.0149 (10)
C13	0.0390 (11)	0.0316 (11)	0.0458 (12)	0.0035 (9)	0.0050 (9)	−0.0164 (9)
C14	0.0330 (10)	0.0300 (10)	0.0353 (10)	−0.0064 (8)	0.0011 (8)	−0.0088 (8)
C15	0.0236 (9)	0.0299 (9)	0.0232 (8)	−0.0022 (7)	0.0042 (7)	−0.0031 (7)
C16	0.0273 (9)	0.0177 (8)	0.0213 (8)	0.0004 (6)	0.0070 (6)	0.0033 (6)
C17	0.0299 (10)	0.0259 (9)	0.0372 (10)	0.0057 (7)	0.0162 (8)	0.0104 (8)
C18	0.0378 (11)	0.0290 (10)	0.0422 (11)	0.0128 (8)	0.0189 (9)	0.0120 (8)
C19	0.0445 (11)	0.0179 (8)	0.0276 (9)	0.0040 (8)	0.0096 (8)	0.0047 (7)
C20	0.0344 (10)	0.0228 (9)	0.0244 (9)	−0.0075 (7)	0.0041 (7)	0.0025 (7)
C21	0.0261 (9)	0.0202 (8)	0.0251 (8)	−0.0031 (7)	0.0045 (7)	0.0015 (7)
C22	0.0159 (7)	0.0200 (8)	0.0275 (8)	−0.0017 (6)	0.0052 (6)	0.0061 (6)
C23	0.0244 (9)	0.0341 (10)	0.0299 (9)	−0.0072 (8)	0.0037 (7)	0.0047 (8)
C24	0.0301 (11)	0.0462 (13)	0.0435 (12)	−0.0152 (9)	−0.0079 (9)	0.0112 (10)
C25	0.0169 (9)	0.0330 (11)	0.0849 (18)	−0.0059 (8)	−0.0030 (10)	0.0166 (11)
C26	0.0194 (9)	0.0298 (11)	0.0860 (18)	−0.0005 (8)	0.0154 (10)	−0.0015 (11)
C27	0.0215 (9)	0.0260 (9)	0.0487 (12)	−0.0016 (7)	0.0116 (8)	−0.0030 (8)
C28	0.0120 (7)	0.0250 (8)	0.0169 (7)	−0.0033 (6)	0.0020 (5)	0.0009 (6)
C29	0.0187 (8)	0.0246 (8)	0.0198 (8)	−0.0039 (6)	0.0006 (6)	0.0003 (6)
C30	0.0313 (10)	0.0295 (9)	0.0242 (9)	−0.0124 (8)	0.0012 (7)	−0.0004 (7)
C31	0.0259 (9)	0.0459 (12)	0.0211 (8)	−0.0176 (8)	−0.0018 (7)	−0.0011 (8)
C32	0.0162 (8)	0.0500 (12)	0.0205 (8)	−0.0067 (8)	−0.0012 (6)	0.0055 (8)
C33	0.0141 (7)	0.0327 (9)	0.0206 (8)	0.0005 (7)	0.0023 (6)	0.0040 (7)
C34	0.0165 (7)	0.0224 (8)	0.0194 (7)	0.0046 (6)	0.0053 (6)	0.0044 (6)
C35	0.0217 (9)	0.0558 (13)	0.0300 (10)	−0.0088 (9)	0.0107 (7)	−0.0091 (9)
C36	0.0230 (10)	0.0792 (18)	0.0408 (12)	−0.0072 (11)	0.0183 (9)	−0.0087 (12)
C37	0.0344 (11)	0.0425 (12)	0.0362 (11)	0.0140 (9)	0.0215 (9)	0.0074 (9)
C38	0.0525 (13)	0.0209 (9)	0.0342 (10)	0.0025 (8)	0.0241 (9)	0.0003 (8)
C39	0.0354 (10)	0.0229 (9)	0.0292 (9)	−0.0037 (7)	0.0164 (8)	−0.0001 (7)
C40	0.0137 (7)	0.0201 (8)	0.0204 (7)	−0.0008 (6)	0.0032 (6)	0.0060 (6)
C41	0.0216 (8)	0.0222 (8)	0.0282 (9)	0.0023 (6)	0.0041 (7)	0.0082 (7)
C42	0.0225 (8)	0.0323 (9)	0.0183 (8)	−0.0008 (7)	0.0038 (6)	0.0042 (7)
C43	0.0121 (7)	0.0212 (8)	0.0173 (7)	−0.0038 (6)	0.0019 (5)	0.0013 (6)
C44	0.0176 (8)	0.0235 (8)	0.0254 (8)	−0.0008 (6)	0.0023 (6)	−0.0017 (7)
C45	0.0255 (9)	0.0316 (10)	0.0322 (10)	−0.0044 (7)	0.0017 (7)	−0.0093 (8)
C46	0.0230 (9)	0.0465 (12)	0.0228 (9)	−0.0071 (8)	−0.0021 (7)	−0.0039 (8)
C47	0.0163 (8)	0.0386 (10)	0.0242 (8)	−0.0003 (7)	−0.0011 (6)	0.0058 (7)
C48	0.0155 (7)	0.0244 (8)	0.0235 (8)	−0.0015 (6)	0.0031 (6)	0.0024 (6)
C49	0.0187 (7)	0.0176 (7)	0.0174 (7)	0.0049 (6)	0.0053 (6)	0.0034 (6)
C50	0.0283 (9)	0.0203 (8)	0.0271 (9)	−0.0006 (7)	0.0107 (7)	−0.0016 (7)
C51	0.0495 (12)	0.0182 (9)	0.0338 (10)	0.0036 (8)	0.0180 (9)	−0.0025 (7)
C52	0.0465 (12)	0.0279 (10)	0.0336 (10)	0.0182 (9)	0.0205 (9)	0.0057 (8)
C53	0.0225 (9)	0.0430 (11)	0.0347 (10)	0.0114 (8)	0.0144 (8)	0.0054 (9)
C54	0.0186 (8)	0.0303 (9)	0.0269 (9)	0.0027 (7)	0.0075 (7)	0.0013 (7)
Co2	0.02194 (11)	0.01939 (11)	0.01954 (11)	−0.00201 (8)	0.00249 (8)	−0.00233 (8)

Cl2	0.0324 (2)	0.0262 (2)	0.0294 (2)	−0.00413 (17)	0.00935 (17)	0.00335 (17)
Cl3	0.0288 (2)	0.0295 (2)	0.0298 (2)	0.00314 (17)	0.00319 (17)	−0.00963 (18)
Cl4	0.0252 (2)	0.0262 (2)	0.02254 (19)	−0.00199 (16)	−0.00564 (15)	−0.00055 (16)

Geometric parameters (Å, º)

Co1—Cl1	2.2398 (4)	C20—C21	1.388 (2)
Co1—P1	2.2241 (5)	C21—H21	0.9500
Co1—P2	2.2260 (4)	C22—C23	1.395 (3)
Co1—P3	2.2653 (4)	C22—C27	1.385 (3)
Co1—P4	2.2913 (4)	C23—H23	0.9500
P1—P2	2.5895 (6)	C23—C24	1.388 (3)
P1—N1	1.7062 (14)	C24—H24	0.9500
P1—C1	1.8242 (17)	C24—C25	1.381 (4)
P1—C10	1.8101 (17)	C25—H25	0.9500
P2—N1	1.6953 (14)	C25—C26	1.368 (4)
P2—C16	1.8175 (17)	C26—H26	0.9500
P2—C22	1.8141 (17)	C26—C27	1.399 (3)
P3—P4	2.6528 (5)	C27—H27	0.9500
P3—N2	1.6935 (13)	C28—C29	1.391 (2)
P3—C28	1.8172 (16)	C28—C33	1.401 (2)
P3—C34	1.8293 (16)	C29—H29	0.9500
P4—N2	1.7137 (13)	C29—C30	1.394 (2)
P4—C43	1.8240 (16)	C30—H30	0.9500
P4—C49	1.8191 (16)	C30—C31	1.384 (3)
N1—C7A	1.500 (6)	C31—H31	0.9500
N1—C7B	1.53 (2)	C31—C32	1.385 (3)
N2—C40	1.5031 (19)	C32—H32	0.9500
C1—C2	1.402 (2)	C32—C33	1.391 (3)
C1—C6	1.395 (2)	C33—H33	0.9500
C2—H2	0.9500	C34—C35	1.400 (2)
C2—C3	1.392 (3)	C34—C39	1.388 (3)
C3—H3	0.9500	C35—H35	0.9500
C3—C4	1.382 (3)	C35—C36	1.394 (3)
C4—H4	0.9500	C36—H36	0.9500
C4—C5	1.393 (3)	C36—C37	1.370 (3)
C5—H5	0.9500	C37—H37	0.9500
C5—C6	1.389 (2)	C37—C38	1.382 (3)
C6—H6	0.9500	C38—H38	0.9500
C7A—H7A	1.0000	C38—C39	1.394 (2)
C7A—C8A	1.531 (7)	C39—H39	0.9500
C7A—C9A	1.519 (7)	C40—H40	1.0000
C8A—H8Aa	0.9800	C40—C41	1.525 (2)
C8A—H8Ab	0.9800	C40—C42	1.527 (2)
C8A—H8Ac	0.9800	C41—H41a	0.9800
C9A—H9Aa	0.9800	C41—H41b	0.9800
C9A—H9Ab	0.9800	C41—H41c	0.9800
C9A—H9Ac	0.9800	C42—H42a	0.9800

C7B—H7B	1.0000	C42—H42b	0.9800
C7B—C8B	1.52 (3)	C42—H42c	0.9800
C7B—C9B	1.50 (2)	C43—C44	1.392 (2)
C8B—H8Ba	0.9800	C43—C48	1.399 (2)
C8B—H8Bb	0.9800	C44—H44	0.9500
C8B—H8Bc	0.9800	C44—C45	1.389 (2)
C9B—H9Ba	0.9800	C45—H45	0.9500
C9B—H9Bb	0.9800	C45—C46	1.384 (3)
C9B—H9Bc	0.9800	C46—H46	0.9500
C10—C11	1.398 (2)	C46—C47	1.385 (3)
C10—C15	1.399 (2)	C47—H47	0.9500
C11—H11	0.9500	C47—C48	1.390 (2)
C11—C12	1.388 (3)	C48—H48	0.9500
C12—H12	0.9500	C49—C50	1.392 (2)
C12—C13	1.386 (3)	C49—C54	1.394 (2)
C13—H13	0.9500	C50—H50	0.9500
C13—C14	1.383 (3)	C50—C51	1.393 (2)
C14—H14	0.9500	C51—H51	0.9500
C14—C15	1.388 (3)	C51—C52	1.382 (3)
C15—H15	0.9500	C52—H52	0.9500
C16—C17	1.392 (3)	C52—C53	1.384 (3)
C16—C21	1.401 (2)	C53—H53	0.9500
C17—H17	0.9500	C53—C54	1.391 (3)
C17—C18	1.390 (3)	C54—H54	0.9500
C18—H18	0.9500	Co2—Cl2	2.2311 (5)
C18—C19	1.385 (3)	Co2—Cl3	2.2275 (5)
C19—H19	0.9500	Co2—Cl4^{i}	2.3433 (5)
C19—C20	1.384 (3)	Co2—Cl4	2.3402 (5)
C20—H20	0.9500		

P1—Co1—Cl1	135.914 (18)	C17—C16—P2	120.20 (13)
P2—Co1—Cl1	91.896 (17)	C21—C16—P2	120.02 (13)
P2—Co1—P1	71.171 (16)	C21—C16—C17	118.86 (16)
P3—Co1—Cl1	97.520 (16)	H17—C17—C16	119.76 (10)
P3—Co1—P1	101.600 (17)	C18—C17—C16	120.49 (17)
P3—Co1—P2	170.583 (18)	C18—C17—H17	119.76 (12)
P4—Co1—Cl1	114.239 (17)	H18—C18—C17	119.91 (12)
P4—Co1—P1	109.466 (17)	C19—C18—C17	120.18 (18)
P4—Co1—P2	105.018 (16)	C19—C18—H18	119.91 (11)
P4—Co1—P3	71.206 (15)	H19—C19—C18	120.10 (11)
P2—P1—Co1	54.449 (14)	C20—C19—C18	119.81 (17)
N1—P1—Co1	94.68 (5)	C20—C19—H19	120.10 (11)
N1—P1—P2	40.27 (5)	H20—C20—C19	119.82 (11)
C1—P1—Co1	110.91 (6)	C21—C20—C19	120.36 (17)
C1—P1—P2	118.53 (6)	C21—C20—H20	119.82 (11)
C1—P1—N1	109.24 (7)	C20—C21—C16	120.23 (17)
C10—P1—Co1	130.28 (6)	H21—C21—C16	119.89 (10)
C10—P1—P2	130.36 (6)	H21—C21—C20	119.89 (11)

C10—P1—N1	104.94 (7)	C23—C22—P2	116.30 (13)
C10—P1—C1	104.92 (8)	C27—C22—P2	124.22 (14)
P1—P2—Co1	54.380 (14)	C27—C22—C23	119.40 (17)
N1—P2—Co1	94.92 (5)	H23—C23—C22	119.87 (11)
N1—P2—P1	40.58 (5)	C24—C23—C22	120.3 (2)
C16—P2—Co1	123.65 (6)	C24—C23—H23	119.87 (14)
C16—P2—P1	123.85 (6)	H24—C24—C23	120.09 (14)
C16—P2—N1	105.35 (7)	C25—C24—C23	119.8 (2)
C22—P2—Co1	116.84 (5)	C25—C24—H24	120.09 (13)
C22—P2—P1	128.36 (6)	H25—C25—C24	119.83 (13)
C22—P2—N1	111.97 (8)	C26—C25—C24	120.34 (19)
C22—P2—C16	103.25 (8)	C26—C25—H25	119.83 (13)
P4—P3—Co1	54.855 (13)	H26—C26—C25	119.78 (13)
N2—P3—Co1	93.87 (5)	C27—C26—C25	120.4 (2)
N2—P3—P4	39.14 (4)	C27—C26—H26	119.78 (14)
C28—P3—Co1	120.07 (5)	C26—C27—C22	119.7 (2)
C28—P3—P4	122.36 (5)	H27—C27—C22	120.15 (11)
C28—P3—N2	108.32 (7)	H27—C27—C26	120.15 (14)
C34—P3—Co1	124.45 (6)	C29—C28—P3	122.64 (12)
C34—P3—P4	130.08 (6)	C33—C28—P3	117.95 (13)
C34—P3—N2	107.87 (7)	C33—C28—C29	119.37 (15)
C34—P3—C28	100.88 (7)	H29—C29—C28	120.07 (9)
P3—P4—Co1	53.939 (13)	C30—C29—C28	119.85 (16)
N2—P4—Co1	92.41 (5)	C30—C29—H29	120.07 (11)
N2—P4—P3	38.60 (4)	H30—C30—C29	119.84 (11)
C43—P4—Co1	120.90 (5)	C31—C30—C29	120.31 (18)
C43—P4—P3	126.52 (5)	C31—C30—H30	119.84 (12)
C43—P4—N2	107.13 (7)	H31—C31—C30	119.80 (12)
C49—P4—Co1	121.87 (5)	C32—C31—C30	120.39 (17)
C49—P4—P3	123.49 (6)	C32—C31—H31	119.80 (10)
C49—P4—N2	108.74 (7)	H32—C32—C31	120.20 (10)
C49—P4—C43	103.85 (7)	C33—C32—C31	119.59 (17)
P2—N1—P1	99.15 (7)	C33—C32—H32	120.20 (11)
C7A—N1—P1	124.4 (3)	C32—C33—C28	120.46 (17)
C7A—N1—P2	133.3 (3)	H33—C33—C28	119.77 (10)
C7B—N1—P1	131.5 (9)	H33—C33—C32	119.77 (11)
C7B—N1—P2	124.4 (9)	C35—C34—P3	121.19 (14)
C7B—N1—C7A	9.2 (10)	C39—C34—P3	120.40 (13)
P4—N2—P3	102.26 (7)	C39—C34—C35	118.41 (16)
C40—N2—P3	124.67 (10)	H35—C35—C34	119.85 (11)
C40—N2—P4	131.97 (10)	C36—C35—C34	120.3 (2)
C2—C1—P1	123.67 (14)	C36—C35—H35	119.85 (13)
C6—C1—P1	117.45 (13)	H36—C36—C35	119.71 (13)
C6—C1—C2	118.86 (16)	C37—C36—C35	120.6 (2)
H2—C2—C1	120.00 (10)	C37—C36—H36	119.71 (12)
C3—C2—C1	120.00 (18)	H37—C37—C36	120.12 (12)
C3—C2—H2	120.00 (12)	C38—C37—C36	119.77 (18)
H3—C3—C2	119.80 (12)	C38—C37—H37	120.12 (12)

C4—C3—C2	120.39 (19)	H38—C38—C37	119.88 (12)
C4—C3—H3	119.80 (12)	C39—C38—C37	120.24 (19)
H4—C4—C3	119.89 (12)	C39—C38—H38	119.88 (12)
C5—C4—C3	120.21 (18)	C38—C39—C34	120.66 (18)
C5—C4—H4	119.89 (12)	H39—C39—C34	119.67 (10)
H5—C5—C4	120.25 (12)	H39—C39—C38	119.67 (12)
C6—C5—C4	119.50 (19)	H40—C40—N2	107.08 (8)
C6—C5—H5	120.25 (12)	C41—C40—N2	112.40 (13)
C5—C6—C1	120.99 (17)	C41—C40—H40	107.08 (9)
H6—C6—C1	119.50 (10)	C42—C40—N2	112.46 (13)
H6—C6—C5	119.50 (12)	C42—C40—H40	107.08 (9)
H7A—C7A—N1	106.3 (2)	C42—C40—C41	110.40 (14)
C8A—C7A—N1	113.7 (4)	H41a—C41—C40	109.5
C8A—C7A—H7A	106.3 (4)	H41b—C41—C40	109.5
C9A—C7A—N1	113.2 (4)	H41b—C41—H41a	109.5
C9A—C7A—H7A	106.3 (2)	H41c—C41—C40	109.5
C9A—C7A—C8A	110.4 (5)	H41c—C41—H41a	109.5
H8Aa—C8A—C7A	109.5	H41c—C41—H41b	109.5
H8Ab—C8A—C7A	109.5	H42a—C42—C40	109.5
H8Ab—C8A—H8Aa	109.5	H42b—C42—C40	109.5
H8Ac—C8A—C7A	109.5	H42b—C42—H42a	109.5
H8Ac—C8A—H8Aa	109.5	H42c—C42—C40	109.5
H8Ac—C8A—H8Ab	109.5	H42c—C42—H42a	109.5
H9Aa—C9A—C7A	109.5	H42c—C42—H42b	109.5
H9Ab—C9A—C7A	109.5	C44—C43—P4	117.79 (12)
H9Ab—C9A—H9Aa	109.5	C48—C43—P4	122.96 (13)
H9Ac—C9A—C7A	109.5	C48—C43—C44	119.19 (15)
H9Ac—C9A—H9Aa	109.5	H44—C44—C43	119.87 (10)
H9Ac—C9A—H9Ab	109.5	C45—C44—C43	120.26 (16)
H7B—C7B—N1	106.0 (9)	C45—C44—H44	119.87 (11)
C8B—C7B—N1	110.4 (18)	H45—C45—C44	119.84 (11)
C8B—C7B—H7B	106.0 (15)	C46—C45—C44	120.33 (18)
C9B—C7B—N1	111.9 (14)	C46—C45—H45	119.84 (11)
C9B—C7B—H7B	106.0 (10)	H46—C46—C45	120.07 (11)
C9B—C7B—C8B	115.8 (18)	C47—C46—C45	119.85 (17)
H8Ba—C8B—C7B	109.5	C47—C46—H46	120.07 (11)
H8Bb—C8B—C7B	109.5	H47—C47—C46	119.87 (11)
H8Bb—C8B—H8Ba	109.5	C48—C47—C46	120.27 (17)
H8Bc—C8B—C7B	109.5	C48—C47—H47	119.87 (11)
H8Bc—C8B—H8Ba	109.5	C47—C48—C43	120.10 (16)
H8Bc—C8B—H8Bb	109.5	H48—C48—C43	119.95 (10)
H9Ba—C9B—C7B	109.5	H48—C48—C47	119.95 (11)
H9Bb—C9B—C7B	109.5	C50—C49—P4	120.93 (13)
H9Bb—C9B—H9Ba	109.5	C54—C49—P4	119.53 (13)
H9Bc—C9B—C7B	109.5	C54—C49—C50	119.03 (15)
H9Bc—C9B—H9Ba	109.5	H50—C50—C49	119.89 (10)
H9Bc—C9B—H9Bb	109.5	C51—C50—C49	120.23 (17)
C11—C10—P1	119.87 (14)	C51—C50—H50	119.89 (12)

C15—C10—P1	121.07 (13)	H51—C51—C50	119.83 (12)
C15—C10—C11	119.07 (16)	C52—C51—C50	120.35 (19)
H11—C11—C10	120.00 (11)	C52—C51—H51	119.83 (12)
C12—C11—C10	120.01 (18)	H52—C52—C51	120.11 (12)
C12—C11—H11	120.00 (12)	C53—C52—C51	119.79 (17)
H12—C12—C11	119.76 (12)	C53—C52—H52	120.11 (11)
C13—C12—C11	120.48 (19)	H53—C53—C52	119.90 (11)
C13—C12—H12	119.76 (12)	C54—C53—C52	120.20 (18)
H13—C13—C12	120.07 (12)	C54—C53—H53	119.90 (12)
C14—C13—C12	119.86 (19)	C53—C54—C49	120.39 (18)
C14—C13—H13	120.07 (12)	H54—C54—C49	119.80 (10)
H14—C14—C13	119.90 (12)	H54—C54—C53	119.80 (12)
C15—C14—C13	120.20 (18)	Cl3—Co2—Cl2	114.33 (2)
C15—C14—H14	119.90 (11)	Cl4—Co2—Cl2	116.502 (19)
C14—C15—C10	120.32 (17)	Cl4^{i}—Co2—Cl2	108.418 (19)
H15—C15—C10	119.84 (10)	Cl4^{i}—Co2—Cl3	114.276 (19)
H15—C15—C14	119.84 (11)	Cl4—Co2—Cl3	110.217 (19)

Co1—P1—N1—P2	−2.33 (4)	N1—P2—C22—C23	179.85 (12)
Co1—P1—N1—C7A	−164.7 (3)	N1—P2—C22—C27	−3.30 (12)
Co1—P1—N1—C7B	−157.2 (12)	N2—P3—C28—C29	6.93 (10)
Co1—P1—C1—C2	−165.49 (11)	N2—P3—C28—C33	−175.19 (11)
Co1—P1—C1—C6	13.05 (9)	N2—P3—C34—C35	−108.20 (13)
Co1—P1—C10—C11	−88.28 (12)	N2—P3—C34—C39	71.75 (12)
Co1—P1—C10—C15	91.49 (11)	N2—P4—C43—C44	−88.44 (10)
Co1—P2—N1—P1	2.33 (4)	N2—P4—C43—C48	88.76 (10)
Co1—P2—N1—C7A	162.2 (3)	N2—P4—C49—C50	30.71 (10)
Co1—P2—N1—C7B	159.7 (11)	N2—P4—C49—C54	−157.50 (11)
Co1—P2—C16—C17	−28.80 (11)	C1—P1—N1—C7A	−50.6 (3)
Co1—P2—C16—C21	162.28 (12)	C1—P1—N1—C7B	−43.2 (12)
Co1—P2—C22—C23	−72.22 (10)	C1—P1—C10—C11	136.49 (12)
Co1—P2—C22—C27	104.64 (12)	C1—P1—C10—C15	−43.73 (11)
Co1—P3—N2—P4	−4.37 (4)	C1—C2—C3—C4	1.7 (2)
Co1—P3—N2—C40	164.90 (8)	C1—C6—C5—C4	1.7 (2)
Co1—P3—C28—C29	112.82 (10)	C2—C1—P1—C10	−20.60 (17)
Co1—P3—C28—C33	−69.29 (9)	C2—C1—C6—C5	0.0 (2)
Co1—P3—C34—C35	143.91 (14)	C2—C3—C4—C5	0.2 (2)
Co1—P3—C34—C39	−36.14 (10)	C3—C2—C1—C6	−1.7 (2)
Co1—P4—N2—P3	4.31 (4)	C3—C4—C5—C6	−1.8 (3)
Co1—P4—N2—C40	−163.80 (9)	C6—C1—P1—C10	157.93 (14)
Co1—P4—C43—C44	15.19 (9)	C7A—N1—P1—C10	61.5 (3)
Co1—P4—C43—C48	−167.60 (11)	C7A—N1—P2—C16	35.3 (4)
Co1—P4—C49—C50	−74.54 (10)	C7A—N1—P2—C22	−76.3 (3)
Co1—P4—C49—C54	97.24 (10)	C7A—N1—C7B—C8B	109 (7)
P1—P2—N1—C7A	159.9 (3)	C7A—N1—C7B—C9B	−21 (8)
P1—P2—N1—C7B	157.4 (11)	C8A—C7A—N1—C7B	−58 (5)
P1—P2—C16—C17	37.88 (11)	C9A—C7A—N1—C7B	69 (5)
P1—P2—C16—C21	−131.04 (11)	C7B—N1—P1—C10	68.9 (12)

P1—P2—C22—C23	−136.63 (12)	C7B—N1—P2—C16	32.8 (11)
P1—P2—C22—C27	40.23 (11)	C7B—N1—P2—C22	−78.7 (11)
P1—N1—P2—C16	−124.57 (8)	C10—C11—C12—C13	−1.6 (2)
P1—N1—P2—C22	123.89 (7)	C10—C15—C14—C13	−0.8 (2)
P1—N1—C7A—C8A	84.5 (5)	C11—C10—C15—C14	−1.5 (2)
P1—N1—C7A—C9A	−148.4 (3)	C11—C12—C13—C14	−0.7 (3)
P1—N1—C7B—C8B	67.4 (16)	C12—C11—C10—C15	2.7 (2)
P1—N1—C7B—C9B	−63.1 (8)	C12—C13—C14—C15	1.9 (3)
P1—C1—C2—C3	176.78 (16)	C16—P2—C22—C23	67.00 (11)
P1—C1—C6—C5	−178.57 (14)	C16—P2—C22—C27	−116.14 (13)
P1—C10—C11—C12	−177.48 (16)	C16—C17—C18—C19	−0.3 (2)
P1—C10—C15—C14	178.68 (15)	C16—C21—C20—C19	1.0 (2)
P2—P1—N1—C7A	−162.3 (3)	C17—C16—P2—C22	−164.36 (15)
P2—P1—N1—C7B	−154.9 (12)	C17—C16—C21—C20	−2.8 (2)
P2—P1—C1—C2	134.56 (12)	C17—C18—C19—C20	−1.5 (3)
P2—P1—C1—C6	−46.90 (10)	C18—C17—C16—C21	2.4 (2)
P2—P1—C10—C11	−14.55 (10)	C18—C19—C20—C21	1.1 (2)
P2—P1—C10—C15	165.23 (13)	C21—C16—P2—C22	26.72 (16)
P2—N1—P1—C1	111.74 (8)	C22—C23—C24—C25	1.1 (2)
P2—N1—P1—C10	−136.21 (7)	C22—C27—C26—C25	1.4 (2)
P2—N1—C7A—C8A	−71.2 (4)	C23—C22—C27—C26	−1.5 (2)
P2—N1—C7A—C9A	55.9 (3)	C23—C24—C25—C26	−1.2 (3)
P2—N1—C7B—C8B	−82.1 (14)	C24—C23—C22—C27	0.2 (2)
P2—N1—C7B—C9B	147.4 (13)	C24—C25—C26—C27	−0.1 (3)
P2—C16—C17—C18	−166.64 (16)	C28—P3—N2—C40	−71.63 (10)
P2—C16—C21—C20	166.30 (14)	C28—P3—C34—C35	5.27 (13)
P2—C22—C23—C24	177.24 (14)	C28—P3—C34—C39	−174.78 (12)
P2—C22—C27—C26	−178.24 (17)	C28—C29—C30—C31	0.4 (2)
P3—P4—N2—C40	−168.11 (9)	C28—C33—C32—C31	0.88 (19)
P3—P4—C43—C44	−50.57 (9)	C29—C28—P3—C34	−106.20 (14)
P3—P4—C43—C48	126.63 (11)	C29—C28—C33—C32	−1.31 (19)
P3—P4—C49—C50	−9.36 (9)	C29—C30—C31—C32	−0.9 (2)
P3—P4—C49—C54	162.42 (12)	C30—C29—C28—C33	0.7 (2)
P3—N2—P4—C43	127.73 (7)	C30—C31—C32—C33	0.2 (2)
P3—N2—P4—C49	−120.60 (7)	C33—C28—P3—C34	71.68 (14)
P3—N2—C40—C41	139.70 (13)	C34—P3—N2—C40	36.76 (10)
P3—N2—C40—C42	−94.96 (13)	C34—C35—C36—C37	−0.1 (3)
P3—C28—C29—C30	178.51 (14)	C34—C39—C38—C37	−0.3 (2)
P3—C28—C33—C32	−179.27 (13)	C35—C34—C39—C38	−1.4 (2)
P3—C34—C35—C36	−178.42 (18)	C35—C36—C37—C38	−1.6 (3)
P3—C34—C39—C38	178.65 (15)	C36—C35—C34—C39	1.6 (3)
P4—P3—N2—C40	169.27 (8)	C36—C37—C38—C39	1.8 (3)
P4—P3—C28—C29	47.70 (9)	C40—N2—P4—C43	−40.38 (15)
P4—P3—C28—C33	−134.42 (11)	C40—N2—P4—C49	71.28 (15)
P4—P3—C34—C35	−145.66 (14)	C43—P4—C49—C50	144.55 (11)
P4—P3—C34—C39	34.29 (10)	C43—P4—C49—C54	−43.67 (11)
P4—N2—P3—C28	119.10 (7)	C43—C44—C45—C46	0.2 (2)
P4—N2—P3—C34	−132.50 (7)	C43—C48—C47—C46	−0.5 (2)

P4—N2—C40—C41	−54.47 (15)	C44—C43—P4—C49	156.58 (13)
P4—N2—C40—C42	70.87 (15)	C44—C43—C48—C47	−0.09 (18)
P4—C43—C44—C45	177.55 (13)	C44—C45—C46—C47	−0.7 (2)
P4—C43—C48—C47	−177.25 (13)	C45—C44—C43—C48	0.2 (2)
P4—C49—C50—C51	172.85 (14)	C45—C46—C47—C48	0.8 (2)
P4—C49—C54—C53	−171.92 (14)	C48—C43—P4—C49	−26.21 (15)
N1—P1—C1—C2	91.46 (12)	C49—C50—C51—C52	−1.6 (2)
N1—P1—C1—C6	−90.00 (11)	C49—C54—C53—C52	−0.5 (2)
N1—P1—C10—C11	21.40 (11)	C50—C49—C54—C53	0.02 (19)
N1—P1—C10—C15	−158.83 (12)	C50—C51—C52—C53	1.1 (2)
N1—P2—C16—C17	78.04 (12)	C51—C50—C49—C54	1.0 (2)
N1—P2—C16—C21	−90.88 (11)	C51—C52—C53—C54	0.0 (2)

Symmetry code: (i) −*x*+1, −*y*, −*z*.